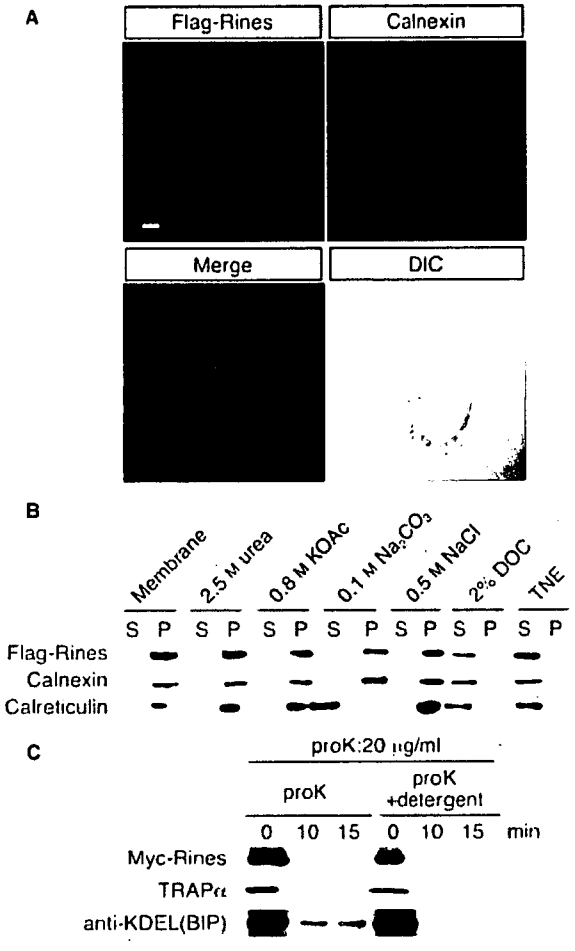

Figure 2 Localization of Rines in cultured cells. (A) Immunofluorescence staining of COS7 cells expressing Flag-Rines. Anti-Calnexin antibody was used to stain a typical ER membrane protein. Blue indicates DAPI-stained nucleus. Scale bar, 5 μm. (B) Membrane preparations of 293T cells expressing Flag-Rines were extracted with buffer containing the materials indicated. *TNE* buffer (150 mM Tris–HCl, pH 7.5; 500 mM NaCl; 1 mM EDTA; 1% Triton X-100; 0.1% SDS), P, pellet; S, supernatant. Each fraction was subjected to immunoblotting with antibodies against Flag-epitope, Calnexin (an integral membrane protein in ER) and Calreticulin (a peripheral membrane protein in ER). (C) N-termini of the Rines are oriented mostly toward the cytoplasm. Protease protection assay of N-terminally Myc-tagged Rines, an ER luminal control *BiP* (Grp78) and an integral ER membrane protein *TRAPα*. The crude membrane fraction prepared from 293T cells expressing Myc-Rines was treated with only proteinase K or with proteinase K with detergent buffer (TNE) for the time indicated. Samples were subjected to immunoblotting using the antibodies indicated.

staining using brains from E13.5 to E17.5 mouse embryos. Throughout these stages, a high level of *Rines* expression was detected in ventricular zone of the lateral ventricle while a low level of expression could be observed throughout other brain region (Fig. 3C–G). At E13.5, the *Rines* expression was detected in a thick layer facing the lateral ventricle, and the expression continued in the ventricular zone at E15.5 through E17.5 (Fig. 3C–G), but the stained layer was thinner at the later stages. In addition, Rines was expressed strongly by lens-forming cells (Fig. 3D). In the sagittal section of E17.5, the *Rines* expression was detected in the olfactory bulb, the ventricular layers facing both on the lateral ventricle and the fourth ventricle and weakly in the thalamus (Fig. 3F). A higher magnification of the cerebral cortex revealed that the *Rines* expression was restricted to the ventricular zone (Fig. 3G).

Rines has a protein-degradation activity dependent on proteasomal function

Because Rines was first found as a Zic2 binding protein in yeast, we performed GST pull-down experiments with the total cell extract from cells transfected with Flag-Rines and GST-fused Zic2 FL (full-length). The precipitates were immunoblotted to detect Flag-Rines (Fig. 4A). We obtained GST-fusion Zic2-bound Rines. To test if the interaction occurs between the purified proteins, we prepared a GST fusion protein containing the Rines fragment obtained from two-hybrid screening (two-hybrid binding region (TBR: 282–489), Fig. 4C) and used this fusion protein for GST pull-down experiments with purified Flag-2HA-Zic2 expressed in, and purified from, 293T cells (Fig. 4B). As a result, we could observe the interaction of GST-Rines-TBR with Flag-2HA-Zic2 (Fig. 4B). This result confirmed that Rines can directly interact with Zic2. Mapping of the Zic2 binding domain in TBR282–489 revealed that both the basic coiled-coil domain and the RING finger domain were involved in the binding (Fig. 4C,D).

To test whether Rines can affect the protein amount of the interacting protein, 293T cells were co-transfected with Flag-Rines and HA-Zic2. We found that the amount of HA-Zic2 in the cell lysate was reduced only when Flag-Rines was co-transfected (Fig. 5A, Input lane2). We then speculated that Rines may be involved in proteasomal protein degradation, because a large number of proteins with the RING finger motif participated in proteasomal protein degradation. This idea led us to examine the HA-Zic2 protein amount in the cells treated with an inhibitor of proteasome function (MG132) or an inhibitor of lysosomal cysteine protease

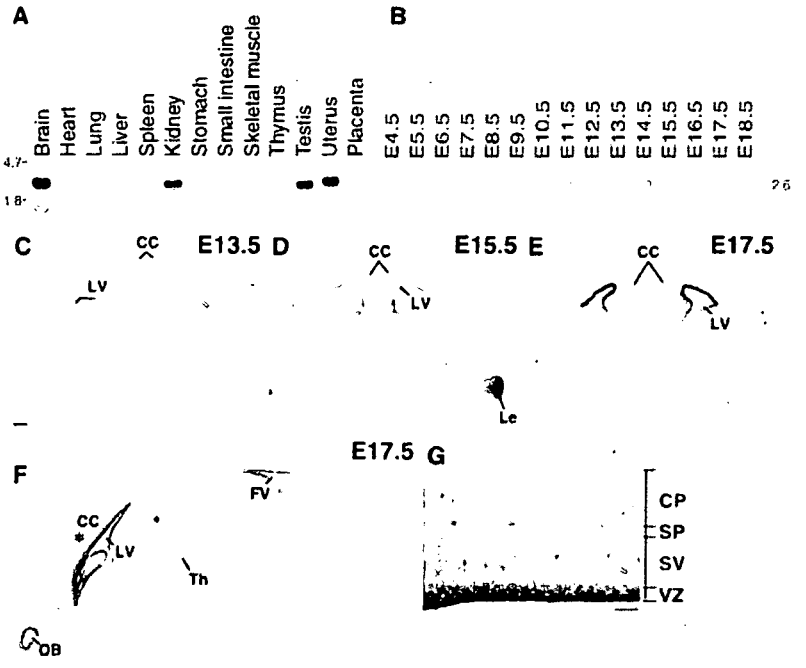

Figure 3 Expression of the Rines. (A–B) Northern blot analyses of a ^{32}P-labeled DNA probe of *Rines*. Each lane contains 20 μg of total RNA. (A) Tissue distribution of the *Rines* mRNA in adult mice. RNA derives from indicated organs of ICR mouse, age 6–10 weeks. (B) Developmental changes in the *Rines* mRNA expression in the mouse embryo from E4.5 to E18.5. (C–G) *in situ* hybridization analysis. *Rines* mRNA distribution is shown in brain sections from E13.5 (C), E15.5 (D), E17.5 (E, F, G) embryos. C–E show coronal sections and F and G show sagittal sections. (G) Higher magnification of the area indicated by asterisk in (F). CC, cerebral cortex; CP, cortical plate; FV, fourth ventricle; Le, lens; LV, lateral ventricle; OB, olfactory bulb; SP, subplate; SV, subventricular zone; Th, thalamus; VZ, ventricular zone. Scale bar, 200 μm.

(E64). As shown in Fig. 5A, the HA-Zic2 in the input lysate decreased in the cells transfected with Flag-Rines was recovered in the cells with MG132 treatment. Similarly, the level of Flag-Rines itself was also increased by the treatment with MG132, but not with E64. In addition, the interaction of Flag-Rines and HA-Zic2 was observed in cells only when the cells were treated with MG132 but not with E64. These results suggest that the apparent absence of the Flag-Rines–HA-Zic2 complex in the cell lysate without MG132 may be due to the rapid degradation of this complex in the proteasome.

To further investigate whether Flag-Rines promotes the degradation of the interacting protein by the proteasome pathway, we examined the Zic2 amount by immunoblot analysis in cells using a series of proteasomal inhibitors or a calpain inhibitor (Fig. 5B). HA-Zic2 was co-transfected into cells with either Flag-Rines or Flag-tagged control vector. The result showed that the Rines-induced degradation of Zic2 was blocked in the presence of the all tested proteasome inhibitors including MG132, Epoxomicin, *clasto*-Lactacystin-β-lactone, Lactacystin and ALLN (Fig. 5B), but was not blocked even in the presence of the high concentration (1 μM) of the calpain inhibitor, Calpastatin peptide (IC50 = 20 nM, Eto *et al.* 1995) (Fig. 5B). These results confirm that Rines promotes the degradation of protein by the proteasome pathway.

To clarify whether or not the Flag-Rines-induced decrement of HA-Zic2 is due to the enhanced Zic2 degradation, we performed a cycloheximide chase experiment. HA-Zic2 was co-expressed in cells with either Flag-Rines or Flag-vector control. Cycloheximide was added 26 h after transfection to inhibit new protein synthesis, and cells were harvested at the indicated time points. The decay of HA-Zic2 was analyzed by immunoblotting. A clear effect on the stability of HA-Zic2 was observed in this cycloheximide chase experiment (Fig. 5C,D). In the presence of the Flag-Rines, the level of HA-Zic2 severely decreased at 4 and 6 h after cycloheximide addition, whereas this effect was not seen in the absence of Flag-Rines. These results indicate that Flag-Rines indeed shortens the half-life of HA-Zic2. We also observed a rapid decrement of Rines itself (Fig. 5C) in accord with the proteasomal degradation of Flag-Rines (Fig. 5A).

Rines can bind to a ubiquitin-conjugating E2 enzyme and shows ubiquitin-ligase activity

The RING finger motifs in RING-type E3s have been shown to serve as recruiting motifs for specific E2 ubiquitin-conjugating enzymes. It was considered that Rines is involved in the proteasomal machinery. To test whether Rines could recruit an E2-ubiquitin conjugating

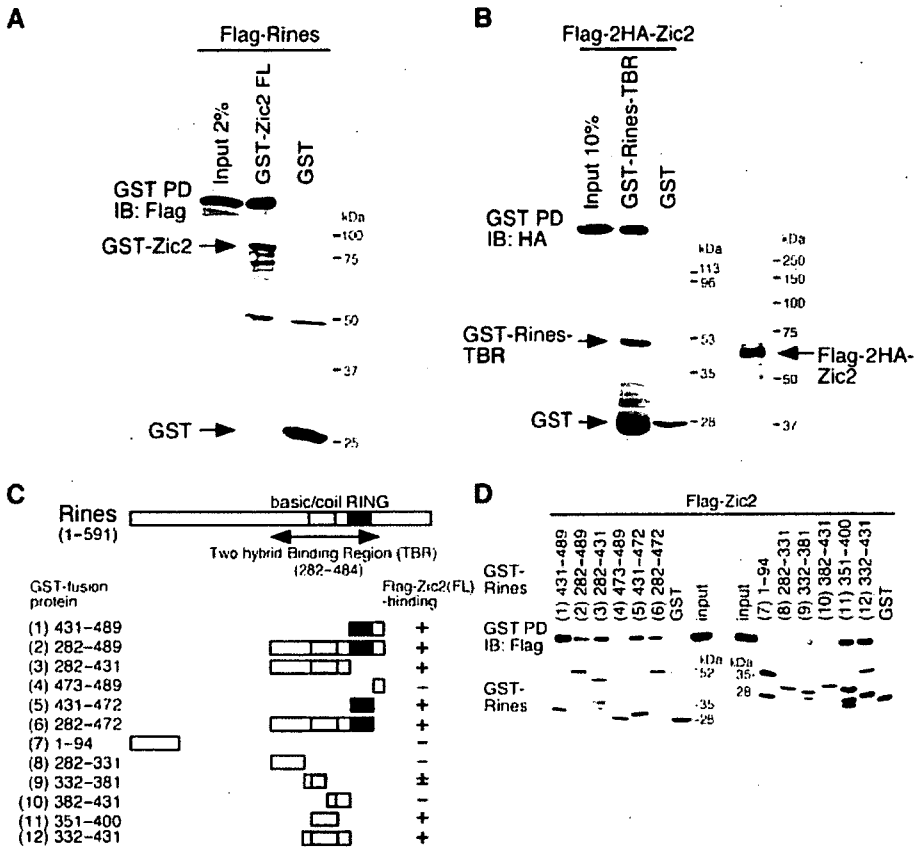

Figure 4 Zic2-binding activity of Rines. (A) Rines binds Zic2 *in vitro*. 293T cells were transfected with Flag-Rines, and the cell lysates containing equal amount of proteins were incubated with the GST-Zic2. The eluates from the glutathione sepharose beads were analyzed by immunoblotting with anti-Flag antibody (upper panel). GST-Zic2 was shown as amido black staining (lower panel). (B) Rines directly interact with Zic2. Flag-2HA-Zic2 expressed and purified from 293T cells was incubated with the GST-Rines-TBR (282–489) fusion protein or GST protein and GST pull-down assay was performed. Bound material was detected by immunoblotting using anti-HA antibody. GST-Rines-TBR fusion protein was shown as amido black staining (lower left panel). The input purified Flag-2HA-Zic2 was shown as silver staining (lower right panel). (C–D) Rines binds Zic2 in the basic coiled-coil domain and RING finger domain. (C) A schematic representation of the Rines, its deletion mutants and the result of mapping of the Zic2-binding region in Rines. The various regions of the Rines were prepared as GST fusion proteins. The numbers refer to amino acids. (D) GST pull-down assays. Upper panel, immunoblot using anti-Flag antibody; lower panel, amido black staining indicating GST-Rines deletion proteins.

enzyme, we performed a GST pull-down assay using GST-Rines-TBR, which contains the RING finger motif, and a set of the Myc-E2s (UbcH5a, H5b, H5 c, H6, H7 and H8) expressed in cells (Fig. 6A). As a result, GST-Rines-TBR associated with Myc-UbcH6, but not with Myc-UbcH5a, H5b, H5c, H7 or H8.

It is known that almost all known RING-type E3 ligases themselves are susceptible to be ubiquitinated (Fang & Weissman 2004). Overexpression of Myc- or Flag-Rines in 293T, NIH 3T3 and COS7 cells resulted in the formation of higher molecular weight bands that were recognized by immunoblot using anti-Myc or Flag antibodies (data not shown). We then examined whether Rines could be covalently modified by ubiquitin (Fig. 6B). An expression plasmid encoding a HA-ubiquitin was transfected into NIH 3T3 cells with or without plasmid for Flag-Rines, followed by immunoprecipitation with anti-Flag antibody. An immunoblot analysis of immunoprecipitates with anti-HA antibody showed a broad band with high molecular weight only when HA-ubiquitin and Flag-Rines were co-expressed. When the same samples were immunoblotted with anti-Flag antibody, the broad bands with high molecular weight appeared regardless of the presence of HA-ubiquitin. These results

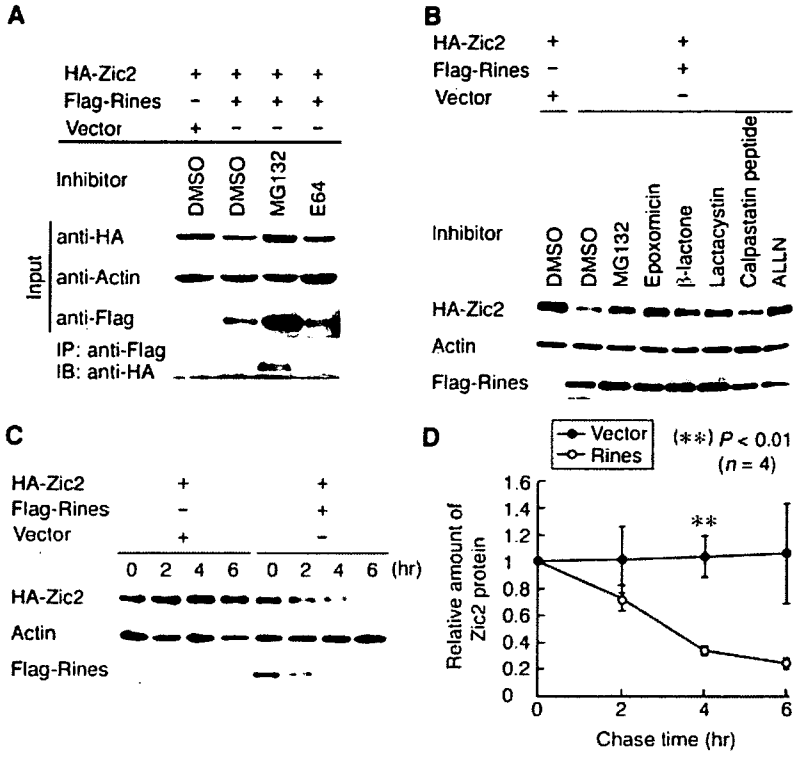

Figure 5 Proteasomal degradation-enhancing activity of Rines. (A) Co-immunoprecipitation of Rines with Zic2 from transfected cells. 293T cells were co-transfected with indicated vectors, and cultured with dimethylsulfoxide (DMSO), proteasome inhibitor MG132 (20 μM), or lysosomal protease inhibitor E64 (50 μM). An equal amount of protein from each cell lysate was subjected to immunoprecipitation and immunoblotting using the antibodies indicated (bottom panel). Expression analysis of the HA-, Flag-tagged gene products and actin protein (as internal control) was done by immunoblotting of the cell extracts (top three panels). The protein ratio used for immunoprecipitation and immunoblotting lanes was 40 : 1. (B) The effects of Rines on Zic2 degradation were blocked by the proteasome inhibitors but not the calpain inhibitor. NIH 3T3 cells were co-transfected with indicated vectors, and were treated with the proteasome inhibitor, MG132 (10 μM), Epoxomicin (10 μM), *clasto*-Lactacystin-β-lactone (10 μM), Lactacystin (20 μM), ALLN (25 μM), the calpain inhibitor, Calpastatine peptide (1 μM) or vehicle (DMSO). The cell lysates were analyzed by immunoblotting. (C–D) Rines accelerates Zic2 turnover. (C) NIH 3T3 cells were transfected with indicated vectors and cultured with cycloheximide. The cell lysates prepared at 0, 2, 4 and 6 h after cycloheximide treatment were analyzed by immunoblotting with anti-HA, anti-Flag or anti-actin antibodies. (D) Relative amount of Zic2. The Zic2 amounts have been normalized to actin so that the value for the amounts at 0 h equals 1.0. The plots indicate means of four independent analyses. Error bars represent standard error. Asterisk denotes statistical significance in the Zic2 amount between the Flag-Rines-transfected and the control vector-transfected cell lysates. **, $P < 0.01$, $n = 4$, by Student's *t*-test.

indicate that Flag-Rines is heavily ubiquitinated and Flag-Rines can be modified with endogenous ubiquitin as well as exogenous ubiquitin.

Next, we tested whether Rines has an ubiquitin ligase activity (Fig. 7A). Flag-Zic2 was co-transfected into NIH 3T3 cells along with HA-tagged ubiquitin in the absence or presence of a plasmid with Myc-tagged Rines. Cell lysates were subjected to immunoprecipitation with an anti-Flag antibody, followed by immunoblotting with an anti-HA antibody to detect ubiquitin-conjugated Zic2. A broad band with high molecular weight was more enhanced in the presence of Myc-Rines than in its absence. Accordingly, the ubiquitination of endogenous Zic2 was enhanced by Myc-Rines in rat neural stem cell line MNS70 cells (Fig. 7B). These results indicate that Rines can promote the polyubiquitination of the interacting protein. Furthermore, deletion of the RING finger motif abolished the ability of Rines to promote the ubiquitination of endogenous Zic2 – the ability integral Rines possesses (Fig. 7B). Because the RING finger motif is suggested to be essential for the enzymatic activity of RING-type E3 ubiquitin ligase (Joazeiro & Weissman

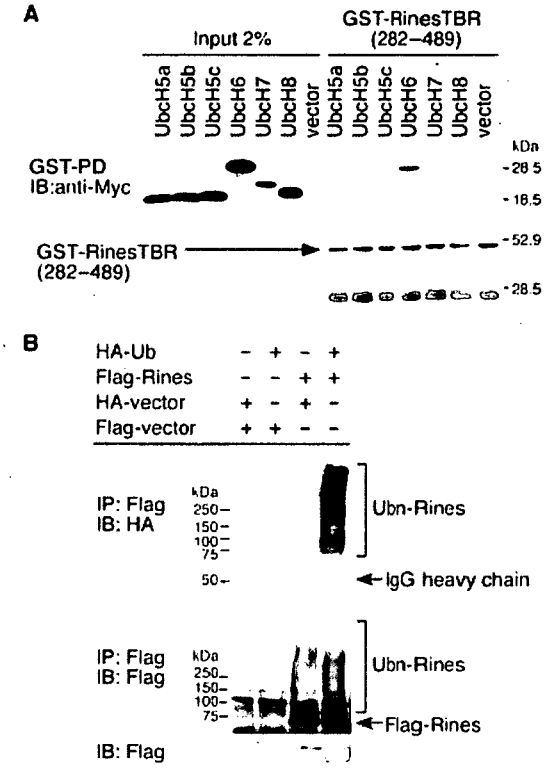

Figure 6 Rines can bind to a ubiquitin-conjugating E2 enzyme and can be polyubiquitinated. (A) Rines binds selectively to UbcH6. Extracts from 293T cells expressing the ubiquitin-conjugating E2 enzymes (Myc-UbcH5a, H5b, H5c, H6, H7, H8) were subjected to GST pull-down assay using the GST-Rines-TBR fusion product, and detected with anti-Myc antibody (upper panel). GST-Rines-TBR fusion product was shown as amido black staining (lower panel). (B) Rines is polyubiquitinated in NIH 3T3 cells. NIH 3T3 cells were transfected with the plasmids indicated. An equal amount of protein from each cell lysate was immunoprecipitated with anti-Flag antibody and then immunoblotted with anti-HA or anti-Flag antibodies to detect ubiquitinated proteins as smear bands (upper two panels). Expression analysis of Flag-Rines by immunoblotting of cell extracts (bottom panel). The protein ratio used for the immunoprecipitation and immunoblotting lanes was 65 : 1.

2000; Pickart 2001), these results support the hypothesis that Rines is an E3 ubiquitin ligase. In addition, we observed the interaction of endogenous Zic2 with both Myc-Rines and Myc-ΔRING (Fig. 7B) in the immunoprecipitation assay. This result is consistent with the *in vitro* binding to Zic2 by Rines (Fig. 4C,D) and the co-immunoprecipitation of Rines with Zic2 (Fig. 5A). These results suggest that Rines can promote the ubiquitination of the interacting protein.

Discussion

Rines gene-encoded product is a novel member of the RING finger protein family and functions as an E3 ubiquitin ligase

Rines contained two functional domains, a C3HC4-type RING finger domain and a basic coiled-coil domain, both of which can act as protein binding domain. As with many other RING-type E3 ligases, the RING finger motif of Rines may function as a recruiting motif for an E2 ubiquitin-conjugating enzyme, UbcH6, because Rines-TBR, which contains the RING finger motif, can bind UbcH6. In addition, the RING finger motif of Rines is required for its protein ubiquitination activity. These results support the inference that Rines functions as an E3 ubiquitin ligase. The coiled-coil domain is known to participate in homo-multimerization of proteins and protein–protein interaction (Jensen *et al.* 2001; Reymond *et al.* 2001). Interestingly, co-existence of the RING domain and the coiled-coil domain is also found in RBCC/TRIM proteins, the RING finger domain of which is similar to that of Rines (Fig. 1C), and in which coiled-coil domains play a role in homo-multimerization and the cell compartment-specific distribution of proteins (Reymond *et al.* 2001; Dho & Kwon 2003). In addition, co-existence of the RING domain and the coiled-coil domain was reported in Staring, which is an E3 ubiquitin ligase targeting syntaxin (Chin *et al.* 2002). In this case, the coiled-coil domain acts as the substrate-binding domain. The finding that the coiled-coil domain can bind a protein is consistent with the macromolecular assembling properties of this domain.

As to the molecular function of Rines, we revealed that Rines functions as an E3 ubiquitin ligase on the basis of the following three facts: (i) Flag-Rines promote the proteasomal degradation of the interacting protein, (ii) Myc-Rines enhance the ubiquitination of the interacting protein, and (iii) GST-Rines-TBR associates with an E2 ubiquitin-conjugating enzyme (Myc-UbcH6). Furthermore, Flag-Rines itself is heavily ubiquitinated and degraded by proteasome as are the case in many other E3 ubiquitin ligase (Fang & Weissman 2004). A rapid degradation of Flag-Rines itself was also observed in cycloheximide chase experiments. This may explain why we could not detect endogenous Rines protein in brain lysates by using anti-Rines antibodies, which could detect over-expressed Rines in cultured cells treated with a proteasome inhibitor (data not shown).

In terms of other molecular properties of Rines, its location in the ER membrane is intriguing. Recent studies of the ER-associated protein degradation (ERAD)

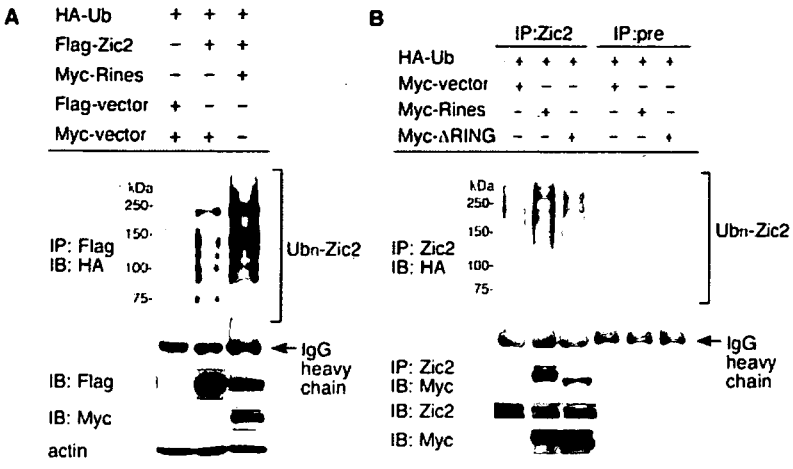

Figure 7 Rines shows ubiquitin-ligase activity. (A) NIH 3T3 cells were transfected with the plasmids indicated. An equal amount of protein from each cell lysate was immunoprecipitated with anti-Flag antibody and then immunoblotted with anti-HA antibody to detect ubiquitinated proteins as smear bands (upper panel). Expression analysis of Flag- and Myc-tagged gene products and actin protein, respectively, by immunoblotting of cell extracts (bottom three panels). The protein ratio used for the immunoprecipitation and immunoblotting lanes was 30 : 1. (B) Rines promotes the ubiquitination of endogenous protein in a RING finger domain-dependent manner. MNS70 cells were transfected with the plasmids indicated and cultured with a proteasome inhibitor (epoxomicin). An equal amount of protein from each cell lysate was immunoprecipitated with anti-Zic2 antibody and then immunoblotted with anti-HA antibody to detect ubiquitinated Zic2 (top panel) and with anti-Myc antibody to detect the interaction of Zic2 and Rines (second from the top panel). Zic2 protein and Myc-tagged Rines in the cell extracts were confirmed by immunoblotting (bottom two panels). The protein ratio used for the immunoprecipitation and immunoblotting lanes was 10 : 1.

system have shown that this system is an essential protein proofreading and elimination system (Kostova & Wolf 2003). Studies in yeast have shown that the RING-finger-domain-containing ER integral membrane proteins Der3/Hrd1p and Doa10 cooperate with an E2 ubiquitin-conjugating enzyme, and they are considered to act as E3 ubiquitin ligases in the ERAD pathway (Bays *et al.* 2001; Deak & Wolf 2001; Swanson *et al.* 2001; Deng & Hochstrasser 2006; Ravid *et al.* 2006). Moreover, RING-finger-domain-containing ER membrane proteins, gp78 and RMA1, are considered to be the mammalian orthologs of the yeast ERAD machinery (Fang *et al.* 2001; Younger *et al.* 2006). The RBCC/TRIM protein RFP2 was recently reported to be an ER membrane anchored ubiquitin ligase involved in the ERAD pathway (Lerner *et al.* 2007). However, it is possible that additional functional homologues exist in vertebrates, considering the increased diversity of functional proteins in vertebrates compared with in yeast. Rines may be a good candidate for a component of the ERAD system in the vertebrate CNS. It is known that Doa10, which resides in the ER/nuclear envelope, degrades the nuclear transcription factor Matα2 as well as ER proteins (Swanson *et al.* 2001; Deng & Hochstrasser 2006; Ravid *et al.* 2006). It is possible that Rines can act in a similar fashion to Doa10 and degrade the substrates of the ERAD pathway as well as nuclear proteins. This possibility should be addressed in a future study.

Possible biological roles of Rines

By using Zic2 as a tool protein that can bind Rines, we demonstrated the proteasomal degradation activity of Rines. However, the biological significance of Rines-mediated Zic2-degradation *in vivo* is unclear, because we did not see a clear increase in Zic2 protein amount in conventional immunoblot or immunofluorescence staining analyses of the brains of *Rines* knockout mice (M. Ogawa and J. Aruga, unpublished observation). Although we cannot exclude the possibility that Rines-mediated Zic2 degradation occurs occasionally, it seems better to postulate that there are other major degradation targets of Rines *in vivo*.

Because the expression of *Rines* is strong in immature neural cells and lens cells, we are interested in the possible degradation targets of Rines in these tissues. In addition, the role of Rines in the nature brain, another major organ showing *Rines* expression, should be clarified.

taking into account emerging roles of the ubiquitin–proteasome pathway in the modulation of neuronal function, such as regulation of synaptic structure and synaptic plasticity (Johnston & Madura 2004; Moriyoshi *et al.* 2004; Yao *et al.* 2007) and in neurodegeneration, such as in Parkinson's disease (Gandhi & Wood 2005) and Alzheimer's disease (Hegde & Upadhya 2007). Although the authentic Rines targets are unclear at this point, the biological significance of Rines is shown by neurobehavioral abnormalities observed in *Rines* knockout mice (M.O., J.A. unpublished observation). Further clarification of the molecular function of Rines is needed for an in-depth understanding of its roles in the proteasomal degradation system in mammalian brains.

Experimental procedures

Yeast two-hybrid screening

Yeast two-hybrid screening was done according to (Mizugishi *et al.* 2004) using an amino-terminal region of mouse Zic2 (amino acid number 1–255) as a bait protein.

cDNA cloning and plasmid construction

Full-length mouse *Rines* cDNA (accession: AAH46775) was cloned by using cDNA library screening and PCR. The cDNA fragment from a cDNA clone obtained in the two-hybrid screening was used for the screening of mouse cerebellum λ-gt11 cDNA library (gifted by Dr T. Furuichi). We obtained the partial cDNA fragment of the *Rines* gene by the screening. Then, 5′ end of the mouse *Rines* cDNA was cloned from E15 mouse embryonic brain cDNAs by using the PCR. The primers used were 5′-TAG CAGCTAATCTCGGTTGC-3′, derived from NCBI database accession:AK013941 and, 5′-GGACATGCACTGATCAGTAA-3′, derived from the cDNA fragment obtained by library screening. The PCR conditions were 35 cycles of 94 °C for 15 min, 58 °C for 1 min and 72 °C for 2 min. The expression vector Flag-Rines was constructed by inserting the entire protein-coding region of *Rines* in-frame into the AviII/SrfI-EcoRI site of pCMVtag2 (Stratagene, La Jolla, CA).

To express Flag-tagged, hemagglutinin (HA)-tagged, and Myc-tagged proteins, the relevant sequences were amplified by PCR, verified by DNA sequencing, and subcloned into pCMVtag2 (Stratagene), pcDNA3HA (a gift from Dr T. Nakajima), and pCS2 + MT (Turner & Weintraub 1994). For the Myc-Rines construct, full-length *Rines* (1–591) was amplified by PCR and digested with *Eco*RI into pCS2 + MT. In the case of Rines-ΔRING-(431–472), two fragments (1–430 and 473–591) amplified by PCR were digested with *Xho*I-*Bgl*I and *Bgl*I-*Xho*I, joined together, and then inserted into pCS2 + MT. The GST-Zic2 was constructed by inserting the cDNA fragment containing the entire ORF of mouse Zic2 into the EcoRI site of pGEX-4T3 vector (GE Healthcare, Uppsala, Sweden). For the GST-Rines-deletions constructs, fragments were amplified by PCR using primers that contain BamHI-EcoRI sites, sequenced, and cloned into the BamHI- EcoRI sites of the pGEX-4T1 vector (GE Healthcare).

HA-Zic2 and Flag-Zic2 were constructed by inserting the cDNA fragment containing the entire ORF of mouse Zic2 into the BamHI-EcoRI site of pcDNA3HA or pCMVtag2 (Mizugishi *et al.* 2001). The Flag-2HA-Zic2 was constructed by inserting the cDNA fragment containing the two tandem repeat of hemagglutinin (HA) into the SrfI-BamHI site of pCMVtag2-Flag-Zic2. The construction of Myc-tagged UbcH5a, H5b, H5c, H6, H7, H8 and HA-tagged Ubiquitin expression vectors will be described elsewhere.

Cell culture and transfection

293T, COS7 and NIH 3T3 cells were maintained at 37 °C with 5% CO_2 in Dulbecco's Modified Eagle's Medium (DMEM, Sigma, St Louis, MO) supplemented with 10% fetal bovine serum (FBS). MNS70 cells (rat neural stem-derived cells, Nakagawa *et al.* 1996) were maintained at 37 °C with 5% CO_2 in a 1 : 1 mixture of DMEM and F12 medium (DF, Sigma) supplemented with 10% FBS, 5% horse serum (HS), and antibiotics. The cells were plated at a density of 3.5×10^4 cells/cm^2 24 h before transfection. 293T and COS7 cells were transfected with Effectene transfection reagent (Qiagen, Valencia, CA) or Trans-IT-LT1 transfection reagent (Mirus, Madison, WI), NIH 3T3 cells were transfected with Superfect transfection reagent (Qiagen) or Lipofectamine Plus or 2000 transfection reagent (Invitrogen, Carlsbad, CA), and MNS70 cells were transfected with Fugene HD transfection reagent (Roche, Basel, Switzerland), according to the manufacturer's instructions.

Immunoblotting

The proteins and gene products were separated by 7.5%–15% SDS-polyacrylamide gel electrophoresis (SDS-PAGE) and transferred to PVDF membrane (Immobilon, Millipore, Bedford, MA). The membranes were immersed in 3%–6% skim milk overnight at 4 °C and incubated with first antibody. The bound antibodies were detected using horseradish peroxidase-conjugated secondary antibodies (anti-mouse, rabbit or rat IgG) and ECL reagents (GE Healthcare).

Subcellular localization studies

COS7 cells were transiently transfected with Flag-Rines. Cells were fixed at 24 h after transfection in 4% paraformaldehyde in 0.1 M sodium phosphate buffer for 15 min at room temperature, incubated with blocking buffer (5% bovine serum albumin in phosphate-buffered saline) for 1 h at room temperature and then incubated overnight at 4 °C with the anti-Calnexin antibody (Stressgen, San Diego, CA) and anti-Flag M2 monoclonal antibody (Sigma) diluted with buffer (0.3% triton X-100 and 1% bovine serum albumin in phosphate-buffered saline). The bound antibodies were detected by Alexa 488-conjugated anti-mouse IgG or Alexa 594-conjugated anti-rabbit IgG antibodies (Molecular Probes Inc., Eugene, OR).

Membrane preparation and protease protection assay

The membrane fraction was prepared as described (Lenk *et al.* 2002). For microsomes of Flag-Rines-transfected 293T cells, cells were scraped 24 h after transfection and then washed once in PBS and homogenized in a homogenization buffer (50 mM Tris–HCl, pH 7.5, 250 mM sucrose, 2 mM EDTA, 150 mM KCl, 1 mM DTT and complete protease inhibitor cocktail (Roche)). The cell lysates were centrifuged at 3000 *g* for 10 min at 4 °C. After centrifugation at 10 000 *g* for 15 min, the supernatant was subsequently centrifuged at 75 000 *g* for 60 min and the pellet (microsome fraction) was resuspended in a membrane buffer (150 mM sucrose, 50 mM Hepes, pH 7.5, 2.5 mM MgOAc, 50 mM KOAc and protease inhibitors) or a membrane buffer containing 2.5 M Urea, 800 mM KOAc, 0.1 M Na_2CO_3, 500 mM NaCl or 2% sodium deoxycholate or TNE buffer (150 mM Tris–HCl, pH 7.5, 500 mM NaCl, 1 mM EDTA, 1% Triton X-100, 0.1% SDS). The cell suspensions were centrifuged at 18 000 *g* for 60 min, then the pellets were resuspended in preboiled SDS-lysis buffer (50 mM Tris–HCl, pH 7.5, 0.5 mM EDTA, 1% SDS, 1 mM dithiothreitol), boiled for an additional 10 min and diluted 10-fold by adding 0.5% NP-40 buffer. A protease protection assay was performed according to the method of Sommer and Jentsch (1993). Myc-Rines-transfected 293T cells were homogenized in the homogenization buffer without EDTA or protease inhibitor and then centrifuged at 3000 *g* for 10 min at 4 °C. The crude homogenates were treated with protease K (20 μg/mL), or untreated, in the presence or absence of detergent buffer (TNE). The following antibodies were used in this study: anti-Flag (M2, Sigma), anti-Myc (9E10, Santa Cruz Biotechnology), anti-Calnexin (BD Biosciences, La Jolla, CA), anti-Calreticulin (BD Biosciences), anti-TRAPα (Upstate, Lake Placid, NY), anti-KDEL (Stressgen).

Northern blot analysis

Two types of Northern blot sheets (Mouse Adult Tissue Blot, Mouse Embryo Full Stage Blot, Seegene, Seoul, Korea) were used to determine the expression profiles of the mouse *Rines* genes. ^{32}P-labeled Rines cDNA probe corresponding to the 1.1 kb fragment of Rines cDNA, from the last RING finger motif toward the 3′untranslated region was synthesized with Random Primed DNA Labeling Kit (Roche). The hybridizations were performed in a buffer consisting of 0.5 M Na_2HPO_4, pH7.2, 7.0% SDS, 1% BSA, 1 mM EDTA, pH8.0, 100 μg/mL herring sperm DNA at 65 °C overnight. These membranes were washed 3 times with 2 × SSC-0.1% SDS at room temperature for 5 min, and finally washed with 0.1 × SSC-0.1% SDS at 56 °C for 40 min, and X-ray films were exposed to the washed membrane with an intensifying screen for 24 h to 7 days. The images were digitized, and the contrast and brightness were optimized.

In situ hybridization

The expression of the *Rines* in the developing animal was investigated in ICR mice purchased from Nihon SLC (Shizuoka, Japan). All animal experiments were carried out according to the guidelines for animal experimentation in RIKEN. *In situ* hybridizations were performed was done as previously described (Nagai *et al.* 1997). Same probe for *Rines* in the Northern blot analysis was used. The specificity of the hybridization signals was verified by the absence of any signals in a control hybridization performed with a *Zic2* sense-strand probe (Nagai *et al.* 1997).

GST pull-down assay

Flag-2HA-Zic2 was purified from 293T cells that were transiently transfected with pCMV-Flag-2HA-Zic2 (Ishiguro *et al.* 2007). Produced protein was affinity-purified with anti-HA agarose beads (Sigma) and HA-peptide (100 ng/mL, Sigma), followed by subsequent affinity purification using anti-Flag agarose beads (Sigma) and Flag-peptide (100 ng/mL, Sigma).

293T cells were transiently transfected with Flag-Rines, Flag-Zic2 or Myc-ubiquitin-conjugating E2 enzyme expression vectors. Cells were harvested 24 h after transfection and were lysed in an immunoprecipitation buffer A (25 mM Hepes, pH 7.2, 0.5% NP-40, 150 mM NaCl, 50 mM NaF, 2 mM Na_3VO_4, 1 mM phenylmethylsulfonyl fluoride, and 20 μg/mL aprotinin) or buffer B (20 mM Hepes, pH 7.4, 150 mM NaCl, 5 mM EDTA, 10% glycerol, 0.5% Triton X-100, 0.5 mM N-ethylmaleimide, 0.5 mM iodoacetamide, 1 mM phenylmethylsulfonyl fluoride and 20 μg/mL aprotinin and contained with 0.1 mg/mL BSA in the case of the direct binding assay). After a centrifugation at 15 000 *g* for 15 min, these supernatant and Flag-2HA-Zic2 were incubated for 2 h at 4 °C with appropriate GST-fusion proteins, and then added with 20 μL of 50% suspension of Glutathione Sepharose 4B beads and incubated for another 2 h at 4 °C. After washing 5 times with the same immunoprecipitation buffer, bound proteins were separated by SDS-PAGE, immunoblotted with the anti-Flag M2 monoclonal antibody (Sigma) or anti-HA Y-11 polyclonal antibody (Santa Cruz Biotechnology, Santa Cruz, CA), or anti-HA 3F10 rat monoclonal antibody (Roche), and detected by ECL system (GE Healthcare).

Immunoprecipitation assay

293T cells were transfected with HA-Zic2 and Flag-Rines or Flag-tagged vector. 48 h after transfection, the cells were treated with the proteasome inhibitor MG132 (Carbobenzoxy-Leu-Leu-Leu-CHO, 20 μM; Calbiochem, San Diego, CA), E64 (50 μM; Sigma) or vehicle Me_2SO; DMSO (final concentration (0.2%)) for 12 h. Cells were then lysed in the immunoprecipitation buffer A (described above) and the lysate was centrifuged at 15 000 *g* for 15 min. These supernatant were incubated for 2 h at 4 °C with a 23 μg of anti-Flag M2 monoclonal antibody (Sigma), and then incubated for another 2 h at 4 °C after adding 20 μL of 50% suspension of protein G agarose beads (Pierce). After washing 5 times with the buffer A, the bound proteins were analyzed by SDS PAGE and immunoblotting as described above.

Degradation assay

NIH 3T3 cells were transfected with HA-Zic2 and Flag-Rines or Flag-tagged control vector. Cells were treated 43 h after transfection

with the proteasome inhibitor, MG132 (10 μM), Epoxomicin (10 μM; Boston Biochem, Cambridge, MA), clasto-Lactacystin-β-lactone (10 μM; BostonBiochem), Lactacystin (20 μM; BostonBiochem or PeptideInstitute, Osaka, Japan), ALLN (Ac-Leu-Leu-Nle-CHO (MG101), 25 μM; Calbiochem), the calpain inhibitor, Calpastatine peptide (1 μM; Calbiochem) or vehicle (DMSO, at a final concentration of 0.2%) for 9 h. The cell lysates were subjected for immunoblotting.

Cycloheximide chase assay

NIH 3T3 cells were transiently co-transfected with HA-Zic2 and Flag-Rines or Flag-tagged vector as described in a degradation assay. 26 h after transfection, culture medium was replaced by DMEM with 10% FBS containing cycloheximide (25 μg/mL). Cells were washed and harvested with PBS(-) buffer 0, 2, 4, 6 h after addition of cycloheximide, lysed and followed by immunoblotting. HA-Zic2 bands and actin bands were densitometrically quantified with NIH Image (v1.61, <http://rsb.info.nih.gov/nih-image/>), and HA-Zic2 amounts were normalized to actin amounts at each time point.

In vivo ubiquitination assay

NIH 3T3 cells were transfected with combinations of the following plasmids: HA-ubiquitin, Flag-Rines, Flag-Zic2, Myc-Rines and Flag-, HA-, Myc-tagged control vectors. After 50 h of incubation, the cells were lysed in a lysis buffer (20 mM Hepes, pH 7.4, 150 mM NaCl, 5 mM EDTA, 10% glycerol, 0.5% Triton X-100, 0.5 mM *N*-ethylmaleimide, 0.5 mM iodoacetamide, and 5 nM ubiquitin aldehyde (Calbiochem)) and a complete protease inhibitor cocktail (Roche). The lysates were subjected to immunoprecipitation by using anti-Flag agarose beads (18 μL, Sigma) and to an immunoblot analysis with anti-HA antibody (Roche) or anti-Flag antibody. For the endogenous Zic2 ubiquitination assay, MNS70 cells were transfected with combinations of the following plasmids: HA-ubiquitin, Myc-Rines, Myc-ΔRING, and Myc-tagged control vector. Forty-three hours after transfection, the cells were incubated for 6 h with 5 μM epoxomicin. The cells lysed in the lysis buffer described above, and the lysates were subjected to immunoprecipitation with anti-Zic2 antibody and immunoblot analysis with anti-HA antibody (Roche).

Acknowledgements

We thank Haruhiko Bito for critical comments on manuscript, Takashi Inoue, Kei-ichi Katayama, Naoko Morimura and Takahiko J Fujimi for technical advice and helpful discussions, members of Aruga and Mikoshiba laboratories for helpful discussions and Shigetsugu Hatakeyama for the gift of HA-ubiquitin vector. This work is supported in parts by The Mochida Memorial Foundation of Medical Pharmaceutical Research, and Grants-in-Aid for Scientific Research from Ministry of Education, Culture, Sports, Science and Technology of Japan.

References

Aruga, J., Nagai, T., Tokuyama, T., Hayashizaki, Y., Okazaki, Y., Chapman, V.M. & Mikoshiba, K. (1996) The mouse *zic* gene family. Homologues of the *Drosophila* pair-rule gene odd-paired. *J. Biol. Chem.* **271**, 1043–1047.

Bays, N.W., Gardner, R.G., Seelig, L.P., Joazeiro, C.A. & Hampton, R.Y. (2001) Hrd1p/Der3p is a membrane-anchored ubiquitin ligase required for ER-associated degradation. *Nat. Cell Biol.* **3**, 24–29.

Borden, K.L. (2000) RING domains: master builders of molecular scaffolds? *J. Mol. Biol.* **295**, 1103–1112.

Chin, L.S., Vavalle, J.P. & Li, L. (2002) Staring, a novel E3 ubiquitin–protein ligase that targets syntaxin 1 for degradation. *J. Biol. Chem.* **277**, 35071–35079.

Deak, P.M. & Wolf, D.H. (2001) Membrane topology and function of Der3/Hrd1p as a ubiquitin–protein ligase (E3) involved in endoplasmic reticulum degradation. *J. Biol. Chem.* **276**, 10663–10669.

Deng, M. & Hochstrasser, M. (2006) Spatially regulated ubiquitin ligation by an ER/nuclear membrane ligase. *Nature* **443**, 827–831.

Dho, S.H. & Kwon, K.S. (2003) The Ret finger protein induces apoptosis via its RING finger-B box-coiled-coil motif. *J. Biol. Chem.* **278**, 31902–31908.

Eto, A., Akita, Y., Saido, T.C., Suzuki, K. & Kawashima, S. (1995) The role of the calpain–calpastatin system in thyrotropin-releasing hormone-induced selective down-regulation of a protein kinase C isozyme, nPKCε, in rat pituitary GH4C1 cells. *J. Biol. Chem.* **270**, 25115–25120.

Fang, S., Ferrone, M., Yang, C., Jensen, J.P., Tiwari, S. & Weissman, A.M. (2001) The tumor autocrine motility factor receptor, gp78, is a ubiquitin protein ligase implicated in degradation from the endoplasmic reticulum. *Proc. Natl. Acad. Sci. USA* **98**, 14422–14427.

Fang, S. & Weissman, A.M. (2004) A field guide to ubiquitylation. *Cell Mol. Life Sci.* **61**, 1546–1561.

Fujiki, Y., Hubbard, A.L., Fowler, S. & Lazarow, P.B. (1982) Isolation of intracellular membranes by means of sodium carbonate treatment: application to endoplasmic reticulum. *J. Cell Biol.* **93**, 97–102.

Gandhi, S. & Wood, N.W. (2005) Molecular pathogenesis of Parkinson's disease. *Hum. Mol. Genet* **14**, 2749–2755.

Giaever, G., Chu, A.M., Ni, L., *et al.* (2002) Functional profiling of the *Saccharomyces cerevisiae* genome. *Nature* **418**, 387–391.

Hegde, A.N. & Upadhya, S.C. (2007) The ubiquitin–proteasome pathway in health and disease of the nervous system. *Trends Neurosci.* **30**, 587–595.

Hershko, A. & Ciechanover, A. (1998) The ubiquitin system. *Annu. Rev. Biochem.* **67**, 425–479.

Hirokawa, T., Boon-Chieng, S. & Mitaku, S. (1998) SOSUI: classification and secondary structure prediction system for membrane proteins. *Bioinformatics* **14**, 378–379.

Ishiguro, A., Ideta, M., Mikoshiba, K., Chen, D.J. & Aruga, J. (2007) Zic2-dependent transcriptional regulation is mediated by DNA-dependent protein kinase, poly(ADP-ribose) polymerase and RNA helicase A. *J. Biol. Chem.* **282**, 9983–9995.

Jensen, K., Shiels, C. & Freemont, P.S. (2001) PML protein isoforms and the RBCC/TRIM motif. *Oncogene* **20**, 7223–7233.

Joazeiro, C.A. & Weissman, A.M. (2000) RING finger proteins: mediators of ubiquitin ligase activity. *Cell* **102**, 549–552.

Johnston, J.A. & Madura, K. (2004) Rings, chains and ladders: ubiquitin goes to work in the neuron. *Prog Neurobiol* **73**, 227–257.

Kostova, Z. & Wolf, D.H. (2003) For whom the bell tolls: protein quality control of the endoplasmic reticulum and the ubiquitin–proteasome connection. *EMBO J.* **22**, 2309–2317.

Lenk, U., Yu, H., Walter, J., Gelman, M.S., Hartmann, E., Kopito, R.R. & Sommer, T. (2002) A role for mammalian Ubc6 homologues in ER-associated protein degradation. *J. Cell Sci.* **115**, 3007–3014.

Lerner, M., Corcoran, M., Cepeda, D., Nielsen, M.L., Zubarev, R., Ponten, F., Uhlen, M., Hober, S., Grander, D. & Sangfelt, O. (2007) The RBCC gene RFP2 (Leu5) encodes a novel transmembrane E3 ubiquitin ligase involved in ERAD. *Mol. Biol. Cell* **18**, 1670–1682.

Mizugishi, K., Aruga, J., Nakata, K. & Mikoshiba, K. (2001) Molecular properties of Zic proteins as transcriptional regulators and their relationship to GLI proteins. *J. Biol. Chem.* **276**, 2180–2188.

Mizugishi, K., Hatayama, M., Tohmonda, T., Ogawa, M., Inoue, T., Mikoshiba, K. & Aruga, J. (2004) Myogenic repressor I-mfa interferes with the function of Zic family proteins. *Biochem. Biophys. Res. Commun.* **320**, 233–240.

Moriyoshi, K., Iijima, K., Fujii, H., Ito, H., Cho, Y. & Nakanishi, S. (2004) Seven in absentia homolog 1A mediates ubiquitination and degradation of group 1 metabotropic glutamate receptors. *Proc. Natl. Acad. Sci. USA* **101**, 8614–8619.

Munoz-Alonso, M.J., Guillemain, G., Kassis, N., Girard, J., Burnol, A.F. & Leturque, A. (2000) A novel cytosolic dual specificity phosphatase, interacting with glucokinase, increases glucose phosphorylation rate. *J. Biol. Chem.* **275**, 32406–32412.

Nagai, T., Aruga, J., Minowa, O., Sugimoto, T., Ohno, Y., Noda, T. & Mikoshiba, K. (2000) Zic2 regulates the kinetics of neurulation. *Proc. Natl. Acad. Sci. USA* **97**, 1618–1623.

Nagai, T., Aruga, J., Takada, S., Gunther, T., Sporle, R., Schughart, K. & Mikoshiba, K. (1997) The expression of the mouse *Zic1*, *Zic2*, and *Zic3* gene suggests an essential role for *Zic* genes in body pattern formation. *Dev Biol.* **182**, 299–313.

Nakagawa, Y., Kaneko, T., Ogura, T., Suzuki, T., Torii, M., Kaibuchi, K., Arai, K., Nakamura, S. & Nakafuku, M. (1996) Roles of cell-autonomous mechanisms for differential expression of region-specific transcription factors in neuroepithelial cells. *Development* **122**, 2449–2464.

Pickart, C.M. (2001) Mechanisms underlying ubiquitination. *Annu. Rev. Biochem.* **70**, 503–533.

Ravid, T., Kreft, S.G. & Hochstrasser, M. (2006) Membrane and soluble substrates of the Doa10 ubiquitin ligase are degraded by distinct pathways. *EMBO J.* **25**, 533–543.

Reymond, A., Meroni, G., Fantozzi, A., Merla, G., Cairo, S., Luzi, L., Riganelli, D., Zanaria, E., Messali, S., Cainarca, S., Guffanti, A., Minucci, S., Pelicci, P.G. & Ballabio, A. (2001) The tripartite motif family identifies cell compartments. *EMBO J.* **20**, 2140–2151.

Rost, B., Fariselli, P. & Casadio, R. (1996) Topology prediction for helical transmembrane proteins at 86% accuracy. *Protein Sci.* **5**, 1704–1718.

Sommer, T. & Jentsch, S. (1993) A protein translocation defect linked to ubiquitin conjugation at the endoplasmic reticulum. *Nature* **365**, 176–179.

Strausberg, R.L., Feingold, E.A., Grouse, L.H., *et al.* (2002) Generation and initial analysis of more than 15 000 full-length human and mouse cDNA sequences. *Proc. Natl. Acad. Sci. USA* **99**, 16899–16903.

Swanson, R., Locher, M. & Hochstrasser, M. (2001) A conserved ubiquitin ligase of the nuclear envelope/endoplasmic reticulum that functions in both ER-associated and Matα2 repressor degradation. *Genes Dev.* **15**, 2660–2674.

Turner, D.L. & Weintraub, H. (1994) Expression of *achaete-scute homolog 3* in *Xenopus* embryos converts ectodermal cells to a neural fate. *Genes Dev.* **8**, 1434–1447.

Yao, I., Takagi, H., Ageta, H., *et al.* (2007) SCRAPPER-dependent ubiquitination of active zone protein RIM1 regulates synaptic vesicle release. *Cell* **130**, 943–957.

Younger, J.M., Chen, L., Ren, H.Y., Rosser, M.F., Turnbull, E.L., Fan, C.Y., Patterson, C. & Cyr, D.M. (2006) Sequential quality-control checkpoints triage misfolded cystic fibrosis transmembrane conductance regulator. *Cell* **126**, 571–582.

Received: 19 September 2007
Accepted: 10 January 2008

Available online at www.sciencedirect.com
ScienceDirect
Neuroscience Research xxx (2008) xxx–xxx
Neuroscience Research
www.elsevier.com/locate/neures

L347P PINK1 mutant that fails to bind to Hsp90/Cdc37 chaperones is rapidly degraded in a proteasome-dependent manner

Yasuhiro Moriwaki [a,b], Yeon-Jeong Kim [b], Yukari Ido [a], Hidemi Misawa [a], Koichiro Kawashima [a], Shogo Endo [c], Ryosuke Takahashi [b,d,*]

[a] *Department of Pharmacology, Kyoritsu University of Pharmacy, 1-5-30 Shibakoen, Minato-ku, Tokyo 105-8512, Japan*
[b] *Laboratory for Motor System Neurodegeneration, RIKEN Brain Science Institute, 2-1 Hiroswa, Wako-Shi, Saitama 351-0198, Japan*
[c] *Unit for Molecular Neurobiology of Learning and Memory, Initial Research Project, Okinawa Institute of Science and Technology, Uruma, Okinawa 904-2234, Japan*
[d] *Department of Neurology, Kyoto University Graduate School of Medicine, 54 Kawahara-cho, Shogoin, Sakyo-ku, Kyoto 606-8507, Japan*

Received 26 November 2007; accepted 15 January 2008

Abstract

Mutation of PTEN-induced kinase 1 (*PINK1*), which encodes a putative mitochondrial serine/threonine kinase, leads to PARK6, an autosomal recessive form of familial Parkinson's disease. Although the precise function(s) of PINK1 protein is unknown, the recessive inheritance of this form of Parkinson's disease suggests loss of PINK1 function is closely associated with its pathogenesis. Here we report that PINK1 forms a complex with the molecular chaperones Hsp90 and Cdc37/p50 within cells, which appears to enhance its stability. When cells were treated with an Hsp90 inhibitor (geldanamycin or novobiocin), levels of PINK1 were greatly diminished, reflecting its rapid degradation via ubiquitin-proteasome pathway. Similarly, the half-life of a pathogenic PINK1 mutant (L347P) that did not interact with Hsp90 or Cdc37/p50 was only 30 min, whereas that of wild-type PINK1 was 1 h. These results strongly suggest that Hsp90 and Cdc37 are binding partners of PINK1 which regulate its stability.

Keywords: Parkinson's disease; PINK1; Hsp90; Cdc37; Proteasome; Stability

1. Introduction

Parkinson's disease (PD) is the second most frequently occurring neurodegenerative disorder and is characterized by selective dopaminergic neural cell loss in the substantia nigra (Dauer and Przedborski, 2003). Most cases of PD are sporadic; in 5–10% of the PD patients, however, the cause is an inherited gene mutation. Moreover, the fact that the clinical characteristics of familial PD are similar to those of sporadic PD has lead to efforts to understand the pathogenic mechanisms induced by the related gene mutations. Several genes are now known to be causally associated with familial PD (Abou-Sleiman et al., 2006). Among them, mutations in the PTEN-induced putative kinase 1 gene (*PINK1*) have been shown to be associated with an autosomal recessive form of familial PD (Valente et al., 2004).

PINK1 was initially isolated from endometrial cancer cells overexpressing PTEN (Unoki and Nakamura, 2001), and the predicted primary sequence of PINK1 protein included an N-terminal mitochondrial-targeting signal along with a catalytic serine/threonine kinase domain. Although PINK1's mitochondrial localization and self-directed phosphorylation activity have already been characterized (Valente et al., 2004; Beilina et al., 2005; Silvestri et al., 2005; Nakajima et al., 2003), its relation to the pathogenesis of PD is poorly understood. However, evidence from several recent studies suggests that PINK1 has the ability to protect cells from stress-induced mitochondrial dysfunction and apoptosis (Valente et al., 2004; Petit et al., 2005; Deng et al., 2005; Park et al., 2006; Clark et al., 2006; Tang et al., 2006). In addition, Deng et al. (2005) recently showed that suppression of PINK1 expression reduces cell viability and significantly increases 1-methyl-4-phenylpyridinium (MPP^+)- and rotenone-induced cytotoxicity. Consistent with those findings, *PINK1*-null flies exhibit male sterility,

* Corresponding author at: Department of Neurology, Kyoto University Graduate School of Medicine, 54 Kawahara-cho, Shogoin, Sakyo-ku, Kyoto 606-8507, Japan. Tel.: +81 75 751 3770; fax: +81 75 761 9780.
E-mail address: ryosuket@kuhp.kyoto-u.ac.jp (R. Takahashi).

0168-0102/$ – see front matter
doi:10.1016/j.neures.2008.01.006

apoptotic muscle degeneration, defects in mitochondrial morphology and increased sensitivity to multiple stresses, including oxidative stress (Park et al., 2006; Clark et al., 2006). These data, along with the recessive nature of *PINK1* mutations, suggest that this form of familial PD is associated with the loss of PINK1 function.

On the other hand, Tang et al. (2006) showed that DJ-1, another protein causatively associated with familial PD, normally interacts with and stabilizes PINK1, and DJ-1 mutations that attenuate this interaction reduce the stability of PINK1. These findings suggest that protein–protein interactions between PINK1 and one or more unknown proteins could play a key regulatory role in affecting the activity and stability of PINK1. In the present study, therefore, we endeavored to isolate PINK1-binding partners using a combination of immunoprecipitation and mass-spectrometric analysis with the aim of obtaining additional information on the pathogenic features of PINK1 mutations. Our findings suggest that the stability of PINK1 is strongly affected by its interaction with Hsp90, and that inhibition of the PINK1–Hsp90 interaction might contribute to the pathogenesis of PD.

2. Materials and methods

2.1. Plasmids and antibodies

The coding region of human PINK1 was cloned using standard RT-PCR techniques. PINK1 mutants were generated using a QuikChange site-directed mutagenesis kit (Stratagene) according to the manufacturer's instructions. Wild-type and all mutant PINK1 cDNAs were cloned into the mammalian expression vector pcDNA3, which also contained the FLAG tag sequence at its 3′ terminal (pcDNA3-FLAG-C). Proper construction of all the plasmids was verified by DNA sequencing. Anti-FLAG (M2), anti-Hsp90 (H-114), anti-Cdc37 (C-11) and anti-HA (Y-11) Abs were purchased from Sigma or Santa Cruz.

2.2. Cell culture and transfection

COS7 and HEK293 cells were cultured in Dulbecco's modified Eagle's medium supplemented with 10% heat-inactivated fetal bovine serum (ICN Biomedical, Inc.), 50 U/ml of penicillin and 50 U/ml of streptomycin at 37 °C under an atmosphere of 95% air/5% CO_2. Plasmids encoding PINK1 cDNAs were transfected into cells using Lipofectamine or Lipofectamine 2000 (Invitrogen) according to the manufacturer's instructions.

2.3. Purification of PINK1-binding proteins

PINK1-FLAG-transfected HEK293 cells were homogenized in lysis buffer (20 mM Hepes [pH 7.4], 150 mM NaCl, 10% glycerol and 1% Triton X-100) supplemented with Complete Protease Inhibitors (Roche Diagnostics). The soluble fraction of the lysate was immunoprecipitated with anti-FLAG M2 agarose (Sigma) and then washed five times in lysis buffer without protease inhibitors. The fractions eluted with 200 μg/ml FLAG peptide were resolved by SDS-PAGE, after which the protein bands were stained with Coomassie Brilliant Blue (CBB) and excised for in-gel digestion.

2.4. Mass-spectral analysis

In-gel digestion was carried out as described by Mineki et al. (2002). Briefly, the excised protein bands were alkylated and then incubated with 12.5 ng/μl trypsin/100 mM NH_4HCO_3 overnight at 37 °C. The resultant tryptic peptides were extracted from the gel by successive incubations with (i) 50% CH_3CN/1% trifluoroacetic acid and (ii) 20% HCOOH/25% CH_3CN/15% isopropanol/40% H_2O. The extracts from each step were pooled and dried by vacuum centrifugation. For peptide mapping, we used a LCQ-Deca XP ion trap mass spectrometer with a nanoelectrospray ionization source (Thermo Electron Corp., Waltham, MA) combined with a reverse-phase capillary column (Cadenza C18, 2 mm × 50 mm, Microme BioResources, Inc., Auburn, CA) on a Magic 2002 high performance liquid chromatography system (Microme BioResources, Inc.). The MS spectra and MS/MS spectra data were collected using Xcalibur software (Matrix Science, London, UK). The data were analyzed for candidate sequences of PINK1-interacting proteins using MASCOT software (Matrix Science) with a public domain protein database (National Center for Biotechnology Information).

2.5. Treatment with Hsp90 and protease inhibitors

Geldanamycin (GA) and novobiocin were purchased from Sigma. Epoxomycin, benzyloxycarbonyl-Leu-Leu-Leu-aldehyde (MG132), pepstatin A and leupeptin were from Peptide Institute. GA (1 mM) was prepared in DMSO and used at a final concentration of 3 μM; novobiocin was prepared in water and used at a final concentration of 1 mM; MG132 (10 mM) was prepared in DMSO and used at a final concentration of 5 μM; epoxomycin (1 mM) was prepared in DMSO and used at a final concentration of 1 μM; leupeptin (1 mM) was prepared in water and used at a final concentration of 20 μM; and pepstatin (1 mM) was prepared in DMSO and used at a final concentration of 25 μM. Cells were exposed to drugs or vehicles 24 h post-transfection.

2.6. Degradation assay

COS7 cells were transiently transfected with wild-type or L347P PINK1-FLAG. Twenty-four hours after transfection, cells were treated with 100 μg/ml cycloheximide (CHX) to prevent protein synthesis, after which they were harvested in lysis buffer at the times indicated in Section 3. Protein concentrations were determined using a Coomassie Plus Protein Assay Reagent kit (Pierce), and equal amounts of protein were subjected to SDS-PAGE. The resolved proteins were transferred to PVDF membranes (Immobilon, Millipore) and analyzed by immunoblot analysis using anti-FLAG Ab, after which the bands were visualized using an enhanced chemiluminescence detection kit (Amersham Pharmacia).

3. Results

3.1. PINK1 forms a complex with both Hsp90 and Cdc37

To isolate PINK1-binding proteins, HEK293 cells were transiently transfected with C-terminal FLAG-tagged PINK1 (PINK1-FLAG), after which proteins in the cell lysates were immunoprecipitated using anti-FLAG M2 agarose, subjected to SDS-PAGE, and stained with CBB. As a control, the same purification procedure was undertaken with non-transfected HEK293 cells. We observed several bands in samples from PINK1-FLAG transfectants that were not discernable in the control sample (Fig. 1A). We then identified the proteins in those bands using standard tryptic peptide mass-spectrometric finger printing (Fig. 1B). Consistent with earlier results, two of the proteins were identified as PINK1, itself (Beilina et al., 2005; Silvestri et al., 2005; Petit et al., 2005; Park et al., 2006), while the others were identified as Hsp90, Hsp70 and Cdc37. Hsp90 and Cdc37 were previously reported to interact with a number of other protein kinases, including one encoded by the PD-related gene *LRRK2* (Gloeckner et al., 2006). We then confirmed the mass-spectral identification of PINK1-associated proteins by immunoblotting samples of the purified protein

Please cite this article in press as: Moriwaki, Y., et al., L347P PINK1 mutant that fails to bind to Hsp90/Cdc37 chaperones is rapidly degraded in a proteasome-dependent manner, Neurosci. Res. (2008), doi:10.1016/j.neures.2008.01.006

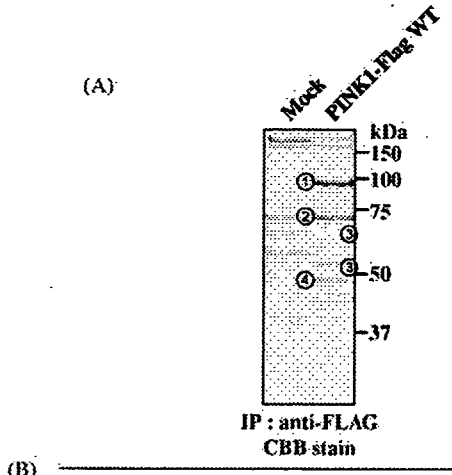

(B)

	Protein name	Score	% sequence converge
①	Hsp90	1623	56 %
②	Hsp70	720	34 %
③	PINK1	917	40 %
④	Cdc37	302	20 %

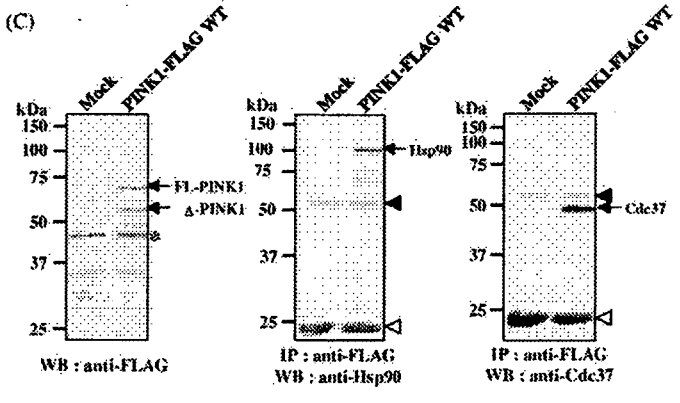

Fig. 1. PINK1 forms a complex with both Hsp90 and Cdc37. (A) HEK293 cells were transfected for 24 h with either a vector expressing PINK1-FLAG or with an empty vector (Mock). The transfectants were then lysed and immunoprecipitated with anti-FLAG Ab, the immunocomplexes were separated by SDS-PAGE, and the gel was stained with CBB to visualize proteins associated with PINK1. (B) CBB stained bands, labeled as indicated in (A), were excised from the gel and, following in-gel digestion with trypsin, their identities were determined by tryptic peptide mass-spectral fingerprinting. Scores and percentages of sequence converge for each protein identified are indicated. (C) The samples purified in (A) were immunoblotted with the indicated Abs; the asterisk indicates a non-specific band detected by anti-FALG Ab. Full length (FL) and processed PINK1 (Δ-PINK1) were detected. Closed and open arrowheads indicate IgG heavy and light chains, respectively.

with Abs against Hsp90, Cdc37 or FLAG (Fig. 1C). Taken together, these findings indicate that Hsp90 and Cdc37 specifically associate with PINK1.

3.2. Hsp90 regulates PINK1 stability

Hsp90 is a ubiquitous molecule that plays a key role in the stabilization and conformational regulation of various signaling effectors, including steroid hormone receptors and protein kinases (Young et al., 2001). To determine whether Hsp90 also regulates PINK1 stability, we next incubated COS7 cells transiently transfected with wild-type PINK1-FLAG with 1–10 μM GA, an inhibitor of Hsp90. We found that cells treated with 1 or 3 μM GA showed reduced levels of PINK1 (Fig. 2, top panel), whereas levels of Hsp90 and Cdc37 were unaffected (Fig. 2, middle and bottom panels). In addition, GA completely blocked the interaction between PINK1 and Hsp90/Cdc37. Examination of the time course of the response to GA revealed that levels of full-length PINK1 gradually declined by 90% over the course of 4 h after the addition of GA to COS7 cells (Fig. 3A). These findings were then confirmed using novobiocin, another known Hsp90 inhibitor that is structurally unrelated to GA and binds to the ATP-binding domain located in the C-terminal part of Hsp90 (Marcu et al., 2000). As shown in Fig. 3A, novobiocin treatment also significantly reduced levels of PINK1 in COS7 cells, and similar results were obtained with HEK293 cells (data not shown). The changes of PINK1 level induced by Hsp90 inhibitors are likely to be ascribable to its protein stability and degradation. First, PINK1 mRNA level was not affected by GA treatment as assessed by RT-PCR analysis (data not shown). Moreover, GA-induced PINK1 downregulation was suppressed by protease inhibitors (Fig. 3B).

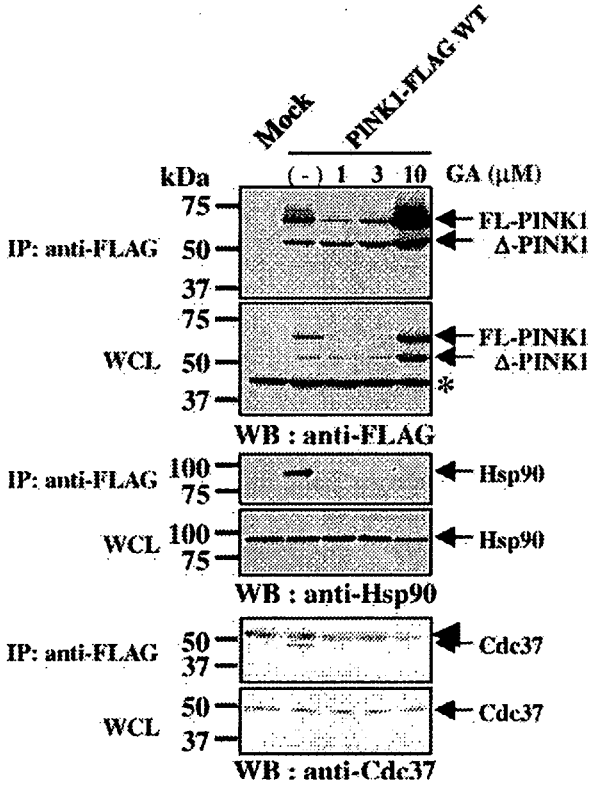

Fig. 2. GA treatment diminishes the interaction of PINK1 with both Hsp90 and Cdc37. COS7 cells were transfected for 24 h with either PINK1-FLAG or Mock expression vector and then treated with indicated concentration of GA. After incubating an additional 4 h, the cells were lysed and immunoprecipitated as described in Section 2. Immunocomplexes and whole-cell lysates (WCLs) were subjected to electrophoresis on polyacrylamide gel and immunoblotted with the indicated Abs; an asterisk indicates a non-specific band detected by anti-FALG Ab, which served as an internal control. The arrowhead indicates IgG heavy chain.

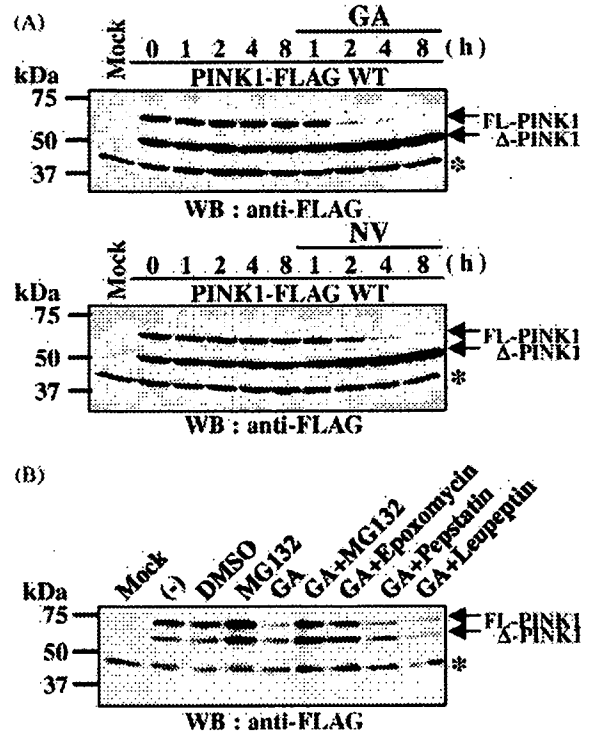

Fig. 3. PINK1 degradation is enhanced by Hsp90 inhibitors but inhibited by proteasome inhibitors. (A) COS7 cells were transiently transfected with PINK1-FLAG, after which the transfectants were incubated for the indicated times in the presence of 3 μM GA, 1 mM novobiocin (NV) or their vehicles (DMSO and water, respectively). After the indicated times or before the addition of drug (T0), the cells were lysed and their lysates were subjected to SDS-PAGE and immunoblotted with anti-FLAG M2 Ab. (B) COS7 cells transiently transfected with PINK1-FLAG were incubated for 4 h in the presence of GA or vehicle (DMSO). The proteasome inhibitors (epoxomycin or MG132) or lysosomal protease inhibitors (pepstatin or leupeptin) were simultaneously added in the presence or absence of GA. (−) indicates no drug treatment; the asterisk indicates a non-specific band detected by anti-FALG Ab, which served as an internal control.

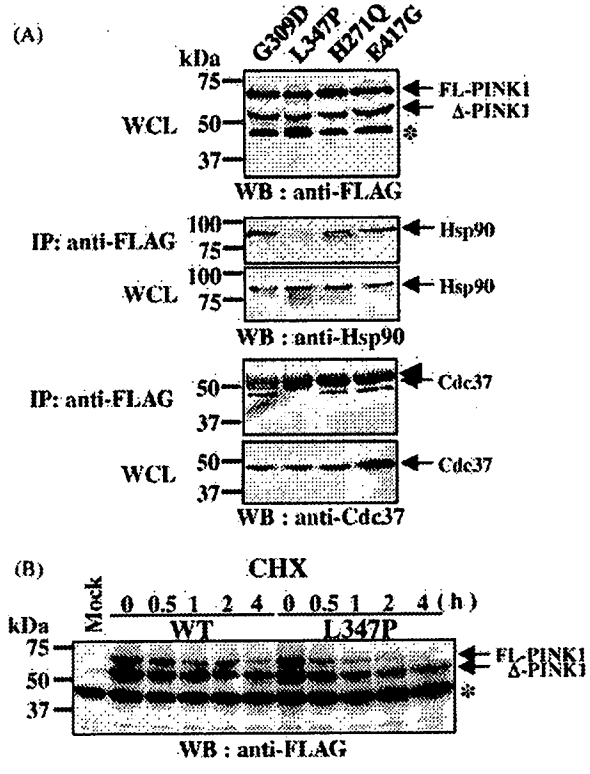

Fig. 4. Familial PD-associated L347P mutation impairs the interaction between PINK1 and Hsp90/Cdc37. (A) Wild-type PINK1 and PD-associated PINK1 mutants expressed in COS7 cells were immunoprecipitated with anti-FLAG Ab and immunoblotted with anti-Hsp90, anti-Cdc37 or anti-FLAG Ab. (B) COS7 cells were transfected for 24 h with either wild-type PINK1-FLAG or L347P mutant PINK1-FLAG, after which they were incubated for the indicated times in the presence of 100 μg/ml cycloheximide (CHX). After the indicated times or before the addition of CHX, cells were resuspended in lysis buffer, and the proteins were analyzed by immunoblotting using anti-FLAG M2 Ab. Similar results were obtained in two independent experiments. The asterisk indicates a non-specific band detected by anti-FALG Ab, which served as an internal control. The arrowhead indicates IgG heavy chain.

Several studies have shown that GA-induced degradation of Hsp90 target proteins is preceded by their ubiquitination and subsequent targeting by proteasome (Miyata et al., 2001; Nony et al., 2003; Boudeau et al., 2003; An et al., 2000). To determine whether GA-mediated decay of PINK1 is also dependent on proteasomal degradation, we blocked proteasome function using two specific inhibitors, epoxomycin and MG132. We found that when COS7 cells expressing PINK1-FLAG were incubated with GA plus either epoxomycin or MG132, but not with other protease inhibitors, degradation of full-length PINK1 was prevented (Fig. 3B). Apparently, upon dissociation of the PINK1–Hsp90 complex, PINK1 is degraded by proteasome.

3.3. Familial PD-associated L347P mutation impairs the interaction between PINK1 and Hsp90/Cdc37

Beilina et al. (2005) recently reported the L347P PINK1 mutant is much more rapidly degraded within cells than wild-type PINK1. To clarify the molecular mechanism underlying the enhanced degradation of the PINK1 mutant, we tested whether PINK1 missense mutants found in familial PD patients (Valente et al., 2004; Hatano et al., 2004) show diminished binding to Hsp90 and/or Cdc37/p50. Immunoprecipitation of PINK1 mutants using anti-FLAG Ab followed by immunoblotting with anti-Hsp90 or Cdc37/p50 Ab revealed that the L347P substitution mutant did not bind to either Hsp90 or Cdc37/p50, whereas the other PD-linked mutations we tested here did not significantly affect the interaction of PINK1 with Hsp90/Cdc37 (Fig. 4A). To confirm the effect of the L347P mutation on protein stability, we also carried out a protein degradation assay and found that the half-life of full-length wild-type PINK1 was 1 h, whereas the half-life of the full-length L347P PINK1 mutant was only 30 min (Fig. 4B). Thus the inability to bind to Hsp90 appears to substantially reduce the stability of the L347P PINK1 mutant.

4. Discussion

Our findings indicate that the molecular chaperone complex Hsp90/Cdc37 bind to PINK1 and thus regulate its stability. Hsp90 is an abundant cytoplasmic protein that functions as a

Please cite this article in press as: Moriwaki, Y., et al., L347P PINK1 mutant that fails to bind to Hsp90/Cdc37 chaperones is rapidly degraded in a proteasome-dependent manner, Neurosci. Res. (2008), doi:10.1016/j.neures.2008.01.006

chaperone and plays an essential role in numerous cellular processes. With fewer target proteins than Hsp60 or Hsp70, Hsp90 appears to primarily bind protein kinases and hormone receptors (Young et al., 2001). To specifically interact with its client proteins, Hsp90 also requires the presence of co-chaperones. One of these, Cdc37/p50, appears to specifically target Hsp90 to a variety of protein kinases, including the mitogen-activated protein kinase (MAPK) family member MAPK-overlapping kinase (MOK) (Miyata et al., 2001), LBK1 (Nony et al., 2003; Boudeau et al., 2003), IKK (Chen et al., 2002) and LRRK2 (Gloeckner et al., 2006). One of the Hsp90/Cdc37 binding proteins IKK was reported to independently bind to both Cdc37 and Hsp90. However, treatment with Hsp90 inhibitors such as GA abolishes the binding ability of IKK to bind both Hsp90 and Cdc37, leading to disruption of its activity. These findings, along with several lines of evidence by the other researchers, suggest that Hsp90 functions in concert with Cdc37 and their interaction is important in their stabilization, activation and/or translocation. Although there is a possibility that Hsp90 and Cdc37 independently bind to PINK1, treatment with Hsp90 inhibitors markedly reduced levels of PINK1 indicate Hsp90/Cdc37 complex are key regulator for PINK1 stability.

Hsp90/Cdc37 interacts with the catalytic domains of several kinases, thereby affecting their enzymatic activity. For example, the interaction of the IKK complex with Hsp90/Cdc37 is required for its activation by tumor necrosis factor (Chen et al., 2002), and the interaction of CDK4 with Hsp90/Cdc37 is required for its proper assembly with cyclin D (Dai et al., 1996). By contrast, the kinase activity of the LKB1 is unaffected by its binding to Hsp90/Cdc37 (Nony et al., 2003). Some recent studies have shown that recombinant PINK1 expressed in *Escherichia coli* has kinase activity (Silvestri et al., 2005; Hatano et al., 2004), but it is not clear whether PINK1 expressed in mammalian cells has similar activity. In our hands, PINK1 exhibited no self-directed phosphorylation activity (data not shown). Further investigation will be required to clarify this issue.

Another function of Hsp90 is stabilization of its target proteins through the prevention of their degradation by the proteasome system. A number of oncogenes, including v-Src (An et al., 2000) and MOK (Miyata et al., 2001), are rapidly degraded in cells following treatment with GA. Consistent with the idea that Hsp90 is a key regulator of PINK1 stability, treatment with Hsp90 inhibitors markedly reduced PINK1 levels within cells (Figs. 2 and 3), while two proteasome inhibitors, epoxomycin and MG132, each prevented Hsp90-inhibitor-induced PINK1 degradation (Fig. 3).

In the present study, we found high concentration of GA treatment conversely augmented PINK1 protein level. Hsp90 was known to form complex with heat shock transcription factor Hsf1, and when this interaction was impaired by adding Hsp90 inhibitor, Hsf1 can form active trimers which enhance the transcription of a subset of genes. According to this idea, other factor(s) induced by Hsf1 may also influence on PINK1 stability.

Beilina et al. (2005) showed that when expressed in either *E. coli* or mammalian cells, steady-state level of the L347P PINK1 mutant is low. They suggested this was the result of enhanced degradation caused by disruption of α-helix similar to that observed in the L166P DJ-1 mutant (Miller et al., 2003). However, we did not observe low steady-state level of L347P PINK1 mutant protein expressed in *E. coli* (data not shown). Instead, the present results suggest that the diminished stability of the L347P PINK1 mutant reflects its inability to interact with Hsp90/Cdc37.

PINK1 reportedly reduces basal neuronal pro-apoptotic activity and protects neurons from staurosporine-induced apoptosis (Silvestri et al., 2005). In addition, Deng et al. (2005) showed that treating cells with PINK1-specific siRNA reduced their viability and significantly increased the cytotoxicity of MPP^+ and rotenone. We found that the L347P mutation diminishes both the interaction of PINK1 with Hsp90 and its stability. These results indicate that L347P mutant PINK1 loses its cell protective function due to destabilization, resulting in the development of PD. Moreover, the present results suggest possible contribution of chaperon system, especially Hsp90, to the pathogenesis of PARK6.

During the preparation of this manuscript, Weihofen et al. (2007) reported that PINK1 interact with Hsp90/Cdc37 complex. They showed GA treatment that affects Hsp90 and client protein interaction preferentially reduced the level of endogenous full-length PINK1. Our findings are consistent with their observations (Figs. 2 and 3). In the present study, we, for the first time, showed that L347P mutant PINK1 displayed diminished interaction with Hsp90/Cdc37, resulting in its instability. Again, these results indicate that L347P mutant PINK1 loses its cell protective function due to destabilization, leading to the development of PD.

Acknowledgements

We thank Dr. Yasuyuki Suzuki for his critical advice and helpful discussions. This study was supported in part by research grants from RIKEN BSI, and a grant-in-aid from the Ministry of Education, Culture, Sports, and Technology of Japan.

References

Abou-Sleiman, P.M., Muqit, M.M., Wood, N.W., 2006. Expanding insights of mitochondrial dysfunction in Parkinson's disease. Nat. Rev. Neurosci. 7, 207–219 review.

An, W.G., Schulte, T.W., Neckers, L.M., 2000. The heat shock protein 90 antagonist geldanamycin alters chaperone association with p210bcr-abl and v-src proteins before their degradation by the proteasome. Cell Growth Differ. 11, 355–360.

Beilina, A., Van Der Brug, M., Ahmad, R., Kesavapany, S., Miller, D.W., Petsko, G.A., Cookson, M.R., 2005. Mutations in PTEN-induced putative kinase 1 associated with recessive parkinsonism have differential effects on protein stability. Proc. Natl. Acad. Sci. U.S.A. 102, 5703–5708.

Boudeau, J., Deak, M., Lawlor, M.A., Morrice, N.A., Alessi, D.R., 2003. Heat-shock protein 90 and Cdc37 interact with LKB1 and regulate its stability. Biochem. J. 370, 849–857.

Chen, G., Cao, P., Goeddel, D.V., 2002. TNF-induced recruitment and activation of the IKK complex require Cdc37 and Hsp90. Mol. Cell 9, 401–410.

Clark, I.E., Dodson, M.W., Jiang, C., Cao, J.H., Huh, J.R., Seol, J.H., Yoo, S.J., Hay, B.A., Guo, M., 2006. Drosophila pink1 is required for mitochondrial function and interacts genetically with parkin. Nature 441, 1162–1166.

Dai, K., Kobayashi, R., Beach, D., 1996. Physical interaction of mammalian CDC37 with CDK4. J. Biol. Chem. 271, 22030–22034.

Dauer, W., Przedborski, S., 2003. Parkinson's disease: mechanisms and models. Neuron 39, 889–909 review.

Deng, H., Jankovic, J., Guo, Y., Xie, W., Le, W., 2005. Small interfering RNA targeting the PINK1 induces apoptosis in dopaminergic cells SH-SY5Y. Biochem. Biophys. Res. Commun. 337, 1133–1138.

Gloeckner, C.J., Kinkl, N., Schumacher, A., Braun, R.J., O'Neill, E., Meitinger, T., Kolch, W., Prokisch, H., Ueffing, M., 2006. The Parkinson disease causing LRRK2 mutation I2020T is associated with increased kinase activity. Hum. Mol. Genet. 15, 223–232.

Hatano, Y., Li, Y., Sato, K., Asakawa, S., Yamamura, Y., Tomiyama, H., Yoshino, H., Asahina, M., Kobayashi, S., Hassin-Baer, S., Lu, C.S., Ng, A.R., Rosales, R.L., Shimizu, N., Toda, T., Mizuno, Y., Hattori, N., 2004. Novel PINK1 mutations in early-onset parkinsonism. Ann. Neurol. 56, 424–427.

Marcu, M.G., Chadli, A., Bouhouche, I., Catelli, M., Neckers, L.M., 2000. The heat shock protein 90 antagonist novobiocin interacts with a previously unrecognized ATP-binding domain in the carboxyl terminus of the chaperone. J. Biol. Chem. 275, 37181–37186.

Miller, D.W., Ahmad, R., Hague, S., Baptista, M.J., Canet-Aviles, R., McLendon, C., Carter, D.M., Zhu, P.P., Stadler, J., Chandran, J., Klinefelter, G.R., Blackstone, C., Cookson, M.R., 2003. L166P mutant DJ-1, causative for recessive Parkinson's disease, is degraded through the ubiquitin-proteasome system. J. Biol. Chem. 278, 36588–36595.

Mineki, R., Taka, H., Fujimura, T., Kikkawa, M., Shindo, N., Murayama, K., 2002. In situ alkylation with acrylamide for identification of cysteinyl residues in proteins during one- and two-dimensional sodium dodecyl sulphate-polyacrylamide gel electrophoresis. Proteomics 2, 1672–1681.

Miyata, Y., Ikawa, Y., Shibuya, M., Nishida, E., 2001. Specific association of a set of molecular chaperones including HSP90 and Cdc37 with MOK, a member of the mitogen-activated protein kinase superfamily. J. Biol. Chem. 276, 21841–21848.

Nakajima, A., Kataoka, K., Hong, M., Sakaguchi, M., Huh, N.H., 2003. BRPK, a novel protein kinase showing increased expression in mouse cancer cell lines with higher metastatic potential. Cancer Lett. 201, 195–201.

Nony, P., Gaude, H., Rossel, M., Fournier, L., Rouault, J.P., Billaud, M., 2003. Stability of the Peutz-Jeghers syndrome kinase LKB1 requires its binding to the molecular chaperones Hsp90/Cdc37. Oncogene 22, 9165–9175.

Park, J., Lee, S.B., Lee, S., Kim, Y., Song, S., Kim, S., Bae, E., Kim, J., Shong, M., Kim, J.M., Chung, J., 2006. Mitochondrial dysfunction in Drosophila PINK1 mutants is complemented by parkin. Nature 441, 1157–1161.

Petit, A., Kawarai, T., Paitel, E., Sanjo, N., Maj, M., Scheid, M., Chen, F., Gu, Y., Hasegawa, H., Salehi-Rad, S., Wang, L., Rogaeva, E., Fraser, P., Robinson, B., St. George-Hyslop, P., Tandon, A., 2005. Wild-type PINK1 prevents basal and induced neuronal apoptosis, a protective effect abrogated by Parkinson disease-related mutations. J. Biol. Chem. 280, 34025–34032.

Silvestri, L., Caputo, V., Bellacchio, E., Atorino, L., Dallapiccola, B., Valente, E.M., Casari, G., 2005. Mitochondrial import and enzymatic activity of PINK1 mutants associated to recessive parkinsonism. Hum. Mol. Genet. 14, 3477–3492.

Unoki, M., Nakamura, Y., 2001. Growth-suppressive effects of BPOZ and EGR2, two genes involved in the PTEN signaling pathway. Oncogene 20, 4457–4465.

Tang, B., Xiong, H., Sun, P., Zhang, Y., Wang, D., Hu, Z., Zhu, Z., Ma, H., Pan, Q., Xia, J.H., Xia, K., Zhang, Z., 2006. Association of PINK1 and DJ-1 confers digenic inheritance of early-onset Parkinson's disease. Hum. Mol. Genet. 15, 1816–1825.

Valente, E.M., Abou-Sleiman, P.M., Caputo, V., Muqit, M.M., Harvey, K., Gispert, S., Ali, Z., Del Turco, D., Bentivoglio, A.R., Healy, D.G., Albanese, A., Nussbaum, R., Gonzalez-Maldonado, R., Deller, T., Salvi, S., Cortelli, P., Gilks, W.P., Latchman, D.S., Harvey, R.J., Dallapiccola, B., Auburger, G., Wood, N.W., 2004. Hereditary early-onset Parkinson's disease caused by mutations in PINK1. Science 304, 1158–1160.

Weihofen, A., Ostaszewski, B., Minami, Y., Selkoe, D.J., 2007. Pink1 Parkinson mutations, the Cdc37/Hsp90 chaperones and Parkin all influence the maturation or subcellular distribution of Pink1. Hum. Mol. Genet. (Epub ahead of print).

Young, J.C., Moarefi, I., Hartl, F.U., 2001. Hsp90: a specialized but essential protein-folding tool. J. Cell Biol. 154, 267–273.

Please cite this article in press as: Moriwaki, Y., et al., L347P PINK1 mutant that fails to bind to Hsp90/Cdc37 chaperones is rapidly degraded in a proteasome-dependent manner, Neurosci. Res. (2008), doi:10.1016/j.neures.2008.01.006

Available online at www.sciencedirect.com
ScienceDirect
Life Sciences 80 (2007) 2206–2209
Life Sciences
www.elsevier.com/locate/lifescie

Ubiquitous expression of acetylcholine and its biological functions in life forms without nervous systems

Koichiro Kawashima [a,*], Hidemi Misawa [a], Yasuhiro Moriwaki [a], Yoshihito X. Fujii [a], Takeshi Fujii [a], Yoko Horiuchi [a], Tomoya Yamada [a], Tadayuki Imanaka [b], Masahiro Kamekura [c]

[a] *Department of Pharmacology, Kyoritsu College of Pharmacy, 1-5-30 Shibakoen, Minato-ku, Tokyo 105-8512, Japan*
[b] *Department of Synthetic Chemistry and Biological Chemistry, Graduate School of Engineering, Kyoto University, Kyoto 606-8501, Japan*
[c] *Noda Institute for Scientific Research, Chiba 278-0037, Japan*

Received 26 September 2006; accepted 26 January 2007

Abstract

Using a radioimmunoassay (RIA) with high specificity and sensitivity (1 pg/tube) for acetylcholine (ACh), we have been able to measure the ACh content in samples from the bacteria, archaea and eucarya domains of the universal phylogenetic tree. We found detectable levels of ACh to be ubiquitous in bacteria (e.g., *Bacillus subtilis*), archaea (e.g., *Thermococcus kodakaraensis* KOD1), fungi (e.g., shiitake mushroom and yeast), plants (e.g., bamboo shoot and fern) and animals (e.g., bloodworm and lugworm). The levels varied considerably, however, with the highest ACh content detected in the top portion of bamboo shoot (2.9 μmol/g), which contained about 80 times that found in rat brain. In addition, using the method of Fonnum, various levels of ACh-synthesizing activity also were detected, a fraction of which was catalyzed by a choline acetyltransferase (ChAT)-like enzyme (sensitive to bromoACh, a selective ChAT inhibitor) in *T. kodakaraensis* KOD1 (15%), bamboo shoot (91%) and shiitake mushroom (51%), bloodworm (91%) and lugworm (81%). Taken together, these findings demonstrate the ubiquitous expression of ACh and ACh-synthesizing activity among life forms without nervous systems, and support the notion that ACh has been expressed and may be active as a local mediator and modulator of physiological functions since the early beginning of life.

Keywords: Acetylcholine; Archaea; Bacteria; Choline acetyltransferase; Eucarya; Radioimmunoassay

Introduction

Although acetylcholine (ACh) is generally known as an important neurotransmitter in the central and peripheral nervous systems of vertebrates and insects, ACh and ACh-synthesizing activity have also been detected in life forms without nervous systems, such as plants, fungi and even bacteria (Horiuchi et al., 2003). Moreover, ACh has been detected in a number of non-neuronal cells in mammalian species, including lymphocytes (see reviews by Kawashima and Fujii, 2000, 2003, 2004); mucocutaneous epithelial keratinocytes (see a review by Grando, 1997); gastrointestinal, respiratory and urogenital epithelial cells (see reviews by Wessler et al., 1998, 2001); and vascular endothelial cells (see a review by Kirkpatrick et al., 2001). These findings suggest that ACh has been expressed from the beginning of life and that, in addition to its role as a neurotransmitter, it serves as a local mediator regulating various physiological functions (Grando et al., 2003; Horiuchi et al., 2003; Wessler et al., 1998).

Wheelis et al. (1992) proposed on the basis of structural features in the small subunit of ribosomal RNA to divide the life on earth into three distinct domains, bacteria, archaea and eucarya. In the present study, we evaluated the ACh content and ACh-synthesizing activity of several representative species

* Corresponding author. Tel.: +81 3 5400 2674; fax: +81 3 5400 2698.
E-mail address: kawashima-ki@kyoritsu-ph.ac.jp (K. Kawashima).

0024-3205/$ - see front matter © 2007 Elsevier Inc. All rights reserved.
doi:10.1016/j.lfs.2007.01.059

from each domain and discussed the potential functions of ACh in life forms without nervous systems.

Materials and methods

Materials

Bacteria: gram-positive bacteria, *Bacillus subtilis* PCI 219. Archaea: thermococcales, *Thermococcus kodakaraensis* KOD1; halophiles, *Haloferax volcanii*. Eucarya: animals (insects), bloodworm (*Chironomus*, larval form); animals (annelids), lugworm (*Marphysa sanguinea*); fungi (Basidiomycota), shiitake mushroom (*Lentinus edodes*, stem portion); fungi (Ascomyta), yeast (*Saccharomyces servisiae*); plants (Anthophyta), bamboo shoot (*Phyllostachys bumbusoides*, top portion); plants (Pterophyta), fern (*Gelichenia gluaca*).

Methods

The ACh content in samples was determined using an RIA as described elsewhere (Horiuchi et al., 2003; Kawashima et al., 1980; Yamada et al., 2005).

ACh-synthesizing activity was determined using a modification of the method of Fonnum (1975) in the presence or absence of 100 μM bromoACh (BrACh), a specific inhibitor of choline acetyltransferase (ChAT) (Tuček, 1982). The ChAT-like activity was defined by subtracting the activity found in the presence of BrACh from that found in the absence of BrACh, and expressed as a percentage of the total ACh-synthesizing activity (Horiuchi et al., 2003; Yamada et al., 2005).

Results

The ACh content

ACh was detected in all of the samples tested from the bacteria, archaea and eucarya domains (Fig. 1). Less ACh was detected in samples of archaea than in samples of eucarya, and bamboo shoot (plants) expressed the highest levels of ACh (about 3 μmol/g). The animals tested (bloodworm and lugworm) expressed ACh at levels comparable to those seen in fungi (shiitake mushrooms and yeast) and plants (fern).

ACh-synthesizing activity

Variable levels of ACh-synthesizing activity were detected in all of the samples tested (Fig. 1), though the activity was not necessarily correlated with the respective ACh contents. For example, samples from shiitake mushroom, yeast and fern showed rather low ACh-synthesizing activities, though their

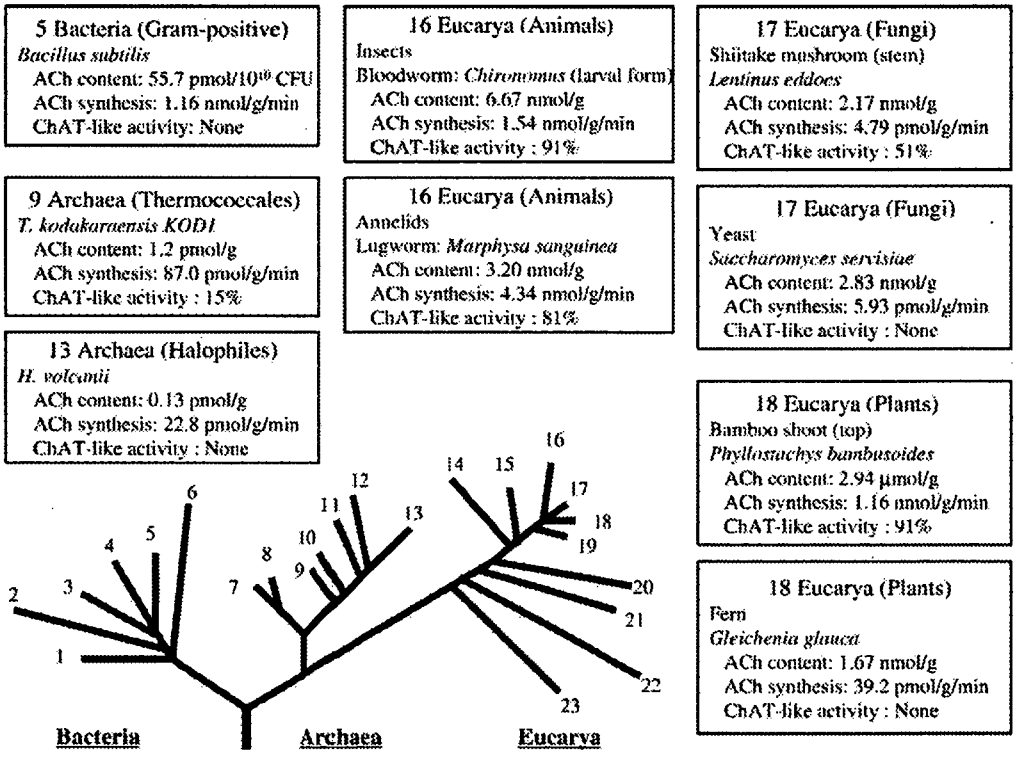

Fig. 1. Expression of acetylcholine (ACh) and ACh-synthesizing activity in representative life forms and the rooted universal phylogenetic tree adopted from Wheelis et al. (1992). Bacteria: 1, thermotogales; 2, flavobacteria and relatives; 3, cyanobacteria; 4, purple bacteria; 5, gram-positive bacteria; and 6, green non-sulfur bacteria. Archaea — kingdom Crenarchaeota: 7, the genus *Pyrodictium*; and 8, the genus *Thermoproteus*; and archaea — kingdom Eurycarhaeota: 9, Thermococcales; 10, Methanococcales; 11, Methanobacteriales; 12, Methanomicrobailes; and 13, extreme halophiles. Eurycarya: 14, entamoebae; 15, slim molds; 16, animals; 17, fungi; 18, plants; 19, ciliates; 20, flagellates; 21, trichomonads; 22, microsporidia; 23, diplomonads. ACh, acetylcholine; CFU, colony forming unit; ChAT, choline acetyltransferase.

ACh contents were quite high. And despite the very high levels of ACh found in bamboo shoot, the observed ACh-synthesizing activity was about the same as in the animals tested (bloodworm and lugworm).

High levels of ChAT-like activity (sensitive to BrACh, a specific ChAT inhibitor) were detected in samples from animals (Fig. 1). In plants, the rapidly growing top portion of bamboo shoot also expressed a high level of ChAT-like activity, but the fern showed no ChAT-like activity at all. In fungi, about 50% of ACh-synthesizing activity in the stem of the shiitake mushroom was ascribed to ChAT-like activity, while no ChAT-like activity was detected in yeast. In archaea, *T. kodakaraensis* KOD1 expressed a small amount of ChAT-like activity.

Discussion

Our present findings, as well as those summarized in our earlier reports (Horiuchi et al., 2003; Yamada et al., 2005), all demonstrate that ACh and the capacity to synthesize ACh are expressed ubiquitously among earth's life forms and suggest that ACh is an evolutionarily old compound, acting as a local mediator and neurotransmitter to regulate various physiological functions.

Although the functions of ACh in life forms without a nervous system are not yet fully understood, it has been suggested that in plants ACh is involved in the regulation of differentiation, water homeostasis and photosynthesis (Wessler et al., 2001). Moreover, on the basis of the asymmetric expression of acetylcholinesterase (AChE) activity in gravi-stimulated maize and rice seedlings and the cloning of AChE from maize (Sagane et al., 2005), Momonoki (1997) and Momonoki et al. (2000) proposed that ACh contributes to the growth of plants by facilitating transport of water and electrolytes. It is also noteworthy that Katsukawa and Shishido (2005) reported that, except in hymenium, there is a higher density of RNA expression in the stipe (stem) of the shiitake mushroom than in the pileus (cap). That the ACh content and the ACh-synthesizing activity are also both higher in the stipe than in the pileus of the shiitake mushroom (Horiuchi et al., 2003) supports the notion that ACh is expressed in activated cells.

Not surprisingly, ACh-synthesizing activity in samples from animals was mostly inhibited by BrACh, suggesting that ACh is mainly synthesized by ChAT in life forms with a nervous system. Nevertheless, Fujii et al. (1995) demonstrated that human T cells express mRNA encoding the same ChAT found in the central nervous system, revealing for the first time that non-neuronal T cells also have the ability to synthesize ACh using ChAT. Furthermore, the specific enhancement of ChAT-catalyzed ACh synthesis seen in phytohemagglutinin-stimulated T cells (Fujii et al., 1996) lent additional support to the idea that ChAT is involved in the ACh synthesis seen in activated non-neuronal cells. Although the specific enzyme catalyzing ACh synthesis in samples from plants and fungi remains to be determined, ChAT-like activity was detected in samples from the rapidly growing top portion of bamboo shoot and the stem of shiitake mushroom, suggesting that ChAT expression also is associated with the growth of plants and fungi. In the flagellated archaeon *T. kodakaraensis* KOD1, weak ChAT-like activity was detected in a sample harvested at the stage of exponential cell growth, suggesting that ACh may be involved in regulating cell growth and/or motility in unicellular organisms.

In summary, ACh and the capacity to synthesize ACh are expressed ubiquitously among life forms without nervous systems. In some organisms, moreover, ChAT-like activity appears to be induced under specific conditions, such as during periods of rapid growth or in response to stressful stimuli. However, the physiological functions of ACh in life forms without nervous systems remain to be clarified.

Acknowledgements

The authors are grateful to Dr. Masako Seki, Dr. Toyoshige Endo, Dr. Takashi Kato, Dr. Tamotsu Kanai, Dr. Taku Amo, Dr. Hiroshi Nishimasu, Dr. Takayoshi Wakagi, and Dr. Hirofumi Shoun for their help and advice.

References

Fonnum, F., 1975. A rapid radiochemical methods for the determination of choline acetyltransferase. Journal of Neurochemistry 24, 407–409.

Fujii, T., Yamada, S., Misawa, H., Tajima, S., Fujimoto, K., Suzuki, T., Kawashima, K., 1995. Expression of choline acetyltransferase mRNA and protein in *t*-lymphocytes. Proceedings of the Japan Academy 71B, 231–235.

Fujii, T., Tsuchiya, T., Yamada, S., Fujimoto, K., Suzuki, T., Kasahara, T., Kawashima, K., 1996. Localization and synthesis of acetylcholine in human leukemic T-cell lines. Journal of Neuroscience Research 44, 66–72.

Grando, S.A., 1997. Biological functions of keratinocyte cholinergic receptors. Journal of Investigative Dermatology Symposium Proceedings 2, 41–48.

Grando, S.A., Kawashima, K., Wessler, I., 2003. Introduction: the non-neuronal cholinergic system in humans. Life Sciences 72, 2009–2012.

Horiuchi, Y., Kimura, R., Kato, N., Fujii, T., Seki, M., Endo, T., Kato, T., Kawashima, K., 2003. Evolutional study on acetylcholine expression. Life Sciences 72, 1745–1756.

Katsukawa, S., Shishido, K., 2005. Analysis of *recQ* gene transcript in fruiting bodies of Basidomycetous mushroom *Lentinula edodes*. Bioscience, Biotechnology and Biochemistry 69, 2247–2249.

Kawashima, K., Fujii, T., 2000. Extraneuronal cholinergic system in lymphocytes. Pharmacology and Therapeutics 86, 29–48.

Kawashima, K., Fujii, T., 2003. Minireview: the lymphocytic cholinergic system and its contribution to the regulation of immune activity. Life Sciences 74, 675–696.

Kawashima, K., Fujii, T., 2004. Expression of non-neuronal acetylcholine in lymphocytes and its contribution to the regulation of immune function. Frontiers in Bioscience 9, 2063–2085.

Kawashima, K., Ishikawa, H., Mochizuki, M., 1980. Radioimmunoassay for acetylcholine in the rat brain. Journal of Pharmacological Methods 3, 115–123.

Kirkpatrick, C.J., Bittinger, F., Unger, R.E., Kriegsman, J., Kilbinger, H., Wessler, I., 2001. The non-neuronal cholinergic system in the endothelium: evidence and possible pathophysiological significance. Japanese Journal of Pharmacology 85, 24–28.

Momonoki, Y.S., 1997. Asymmetric distribution of acetylcholinesterase in gravistimulated maize seedlings. Plant Physiology 114, 47–53.

Momonoki, Y.S., Kawai, N., Takamure, I., Kowalczk, S., 2000. Gravitropic response of acetylcholinesterase and IAA-inositol synthase in lazy rice. Plant Production Science 3, 17–23.

Sagane, Y., Nakagawa, T., Yamamoto, K., Michikawa, S., Oguri, S., Momonoki, Y.S., 2005. Molecular characterization of maize acetylcholinesterase. A novel enzyme family in the plant kingdom. Plant Physiology 138, 1359–1371.

Tuček, S., 1982. The synthesis of acetylcholine in skeletal muscles of the rat. Journal of Physiology (London) 322, 53–69.

Wessler, I., Kirkpatrick, C.J., Racké, K., 1998. Non-neuronal acetylcholine, a locally acting molecule widely distributed in biological system: expression and function in humans. Pharmacology and Therapeutics 77, 59–79.

Wessler, I., Kilbinger, H., Bittinger, F., Kirkpatrick, C.J., 2001. The biological role of non-neuronal acetylcholine in plants and humans. Japanese Journal of Pharmacology 85, 2–10.

Wheelis, M.L., Kandler, O., Woese, C.R., 1992. On the nature of global classification. Proceedings of the National Academy of Sciences of the United States of America 89, 2930–2934.

Yamada, T., Fujii, T., Kanai, T., Amo, T., Imanaka, T., Nishimasu, H., Wakagi, T., Shoun, H., Kamekura, M., Kamagata, Y., Kato, T., Kawashima, K., 2005. Expression of acetylcholine (ACh) and ACh-synthesizing activity in Archaea. Life Sciences 77, 1935–1944.